CALIFORNIA PATH PROGRAM
INSTITUTE OF TRANSPORTATION STUDIES
UNIVERSITY OF CALIFORNIA, BERKELEY

Vehicle Following Control Design for Automated Highway Systems

H. Raza
P. Ioannou
University of Southern California

California PATH Research Report
UCB-ITS-PRR-97-2

This work was performed as part of the California PATH Program of the University of California, in cooperation with the State of California Business, Transportation, and Housing Agency, Department of Transportation; and the United States Department of Transportation, Federal Highway Administration.

January 1997

ISSN 1055-1425

Vehicle Following Control Design €or Automated Highway Systems

by

H. **Raza,** P. Ioannou

Vehicle Following Control Design for Automated Highway Systems*

H. Raza and P. Ioannou
Dept. of Electrical Engineering-Systems
University of Southern California
Los Angeles, CA 90089-2562

Abstract.

Automatic vehicle following is an important feature of a fully or partially automated highway system **(AHS).** The on-board vehicle control system should be able to accept and process inputs from the driver, the infrastructure and other vehicles, perform diagnostics and provide the appropriate commands to actuators so that the resulting motion of the vehicle is safe and compatible with the AHS objectives. The purpose of this paper is to design and test a vehicle control system in order to achieve full vehicle automation in the longitudinal direction for several modes of operation, where the infrastructure manages the vehicle following. These modes include autonomous vehicles, cooperative vehicle following and platooning. The vehicle control system consists of a supervisory controller that processes the inputs from the driver, the infrastructure, other vehicles and the on-board sensors and sends the appropriate commands to the brake and throttle controllers. In addition, the controller makes decisions about normal, emergency and transition operations. Simulation results of some of the basic vehicle following maneuvers are used to verify the claimed performance of the designed controllers. Experiments on 1-15 that demonstrate the performance of the throttle controller with and without vehicle-to-vehicle communications in an actual highway environment are also included.

Keywords: Vehicle Control, Automated Highway Systems, Automatic Vehicle Following, Supervisory Control.

*This work is supported by the California Department of Transportation through PATH of the University of California. The contents of this paper reflect the views of the authors who are responsible for the facts and the accuracy of the data presented herein. The contents do not necessarily reflect the official views or policies of the State of California. This paper does not constitute a standard, specification or regulation.

Executive Summary

In this report the problem of design of on-board vehicle intelligence for achieving full vehicle automation in the longitudinal direction is addressed. The on-board intelligence is an essential part of any vehicle following scheme for a fully or partially automated highway system to provide the necessary interface between the vehicle subsystem controllers and the external agents.

A supervisory controller is designed to provide the required intelligence for several modes of operation of infrastructure managed vehicle following. The supervisory controller processes the inputs from the driver, the infrastructure, surrounding vehicle and on-board sensors and sends the appropriate commands to the brake and throttle controllers. It makes decisions about normal, emergency and transition operations so that the resulting motion of vehicle is safe and follows AHS objectives. Simulation results are used to test the performance of the designed controllers. Finally, the experimental results of a vehicle following test conducted on 1-15 demonstrates the effectiveness of the controller in an actual highway environment.

Contents

List of Figures

1 Introduction

One of the objectives of Automated Highway Systems **(AHS)** is to meet the increasing demand for capacity by the efficient utilization of the existing infrastructure. Capacity is calculated by the simple formula:

$$C = \frac{V}{X_r + L} \tag{1}$$

where C is the capacity, measured in number of vehicles crossing a fixed point/unit time, V is the vehicular speed of flow, X_r is the inter-vehicle spacing and L is the vehicle length. The capacity formula **(1)** is derived by assuming that all vehicles have the same length L, keep the same inter-vehicle spacing X_r and follow the same speed V. The capacity C can be viewed **as** the maximum possible flow rate q for a given speed V, inter-vehicle spacing X, and vehicle length L. While the traffic flow rate may exceed C during transients by violating the maximum allowable V or minimum allowable X_r, in an AHS environment such violations have to be reduced or eliminated for safety considerations. Therefore in AHS q has to be kept less than or equal to C during transients and C should be the desired value q should converge to in steady state. These constraints give rise to the following requirements:
(i) The system should be designed for maximum capacity under the constraints of safety.
(ii) The system should be designed so that the actual traffic flow rates tend to the maximum capacity at steady state and transients are not excessive and are not due to the violation of safety constraints on the vehicle level.

The first requirement can be met by using the safety considerations to decide about the maximum allowable speed V and minimum inter-vehicle spacing X_r [1]. The second requirement can be met by designing the vehicle following control system properly, getting the infrastructure involved in managing traffic **flow** on the macroscopic level, minimizing disturbances due to lane changing and by choosing the appropriate configurations for the roadway system [2, **3,** 5].

The purpose of this paper is to concentrate on the design of the vehicle longitudinal control system (VLCS) that will guarantee smooth and safe vehicle following. In an AHS environment the VLCS should be able to accept and process inputs from the driver, infrastructure, other vehicles in the vicinity **as** well **as** from its own sensors. The VLCS is designed for intelligent cruise control (ICC) applications, cooperative driving and platooning. In ICC the vehicle is autonomous in the sense that it does not communicate with the infrastructure and/or other vehicles. In cooperative driving the VLCS may accept inputs from the vehicles in front and the infrastructure, whereas in platooning the VLCS has to process inputs from the leader of the platoon **as** well **as** from the infrastructure and other vehicles. These three different modes of operation may be necessary in AHS and the design of a VLCS to operate in each chosen mode is therefore essential.

The VLCS consists of a supervisory controller which is the "brain" of the system and a throttle/brake controller. Since several throttle/brake controllers have already been proposed and tested [6-11], the emphasis of the paper is on the supervisory controller and its interaction with the various inputs and throttle/brake controller. The design of the supervisory controller is similar to the design concept of event driven state machine control. The design objective is to replace the human driver functions in the longitudinal direction. The throttle and brake controllers are used both in normal as well as in emergency situation to give complete automation in the longitudinal direction.

The emergency situation handling logic, as a part of the supervisory controller, is designed on the principles used by the human drivers to handle emergencies. It comprises a situation assessment logic to detect the presence of emergencies, and a compensation logic to handle emergencies of different severities. The effectiveness of this scheme relies on the quality of the sensors and actuators that can provide low detection and actuation delays. In addition, the supervisory controller chooses the mode of operation and handles the transitions from manual to automatic and vice-versa.

The paper is organized as follows: Some of the possible AHS configurations are discussed in section 2. The concept of vehicle longitudinal control design and a detailed description of the design of supervisory controller is presented in section 3. The stability and performance analysis of the overall closed loop system is given in section 4. A sufficient condition for stability of platoon of vehicles is developed in the same seciton. In section 5, the simulation and experimental results for different vehicle following scenarios are discussed. The paper ends with the main results summarized in the conclusion section.

Basic Notation

AVF	automatic vehicle following
ICC	intelligent cruise control
VLCS	vehicle longitudinal control system
a	acceleration of the vehicle (m/sec^2)
h	time headway (sec)
V	speed of the vehicle (m/sec)
$\mathcal{B}_{sub}$	boolean variables, *sub* identifies each variable
h_{sub}	variables associated with headway
V_{sub}	variables associated with speed

2 AHS Configuration and Modes of Operation

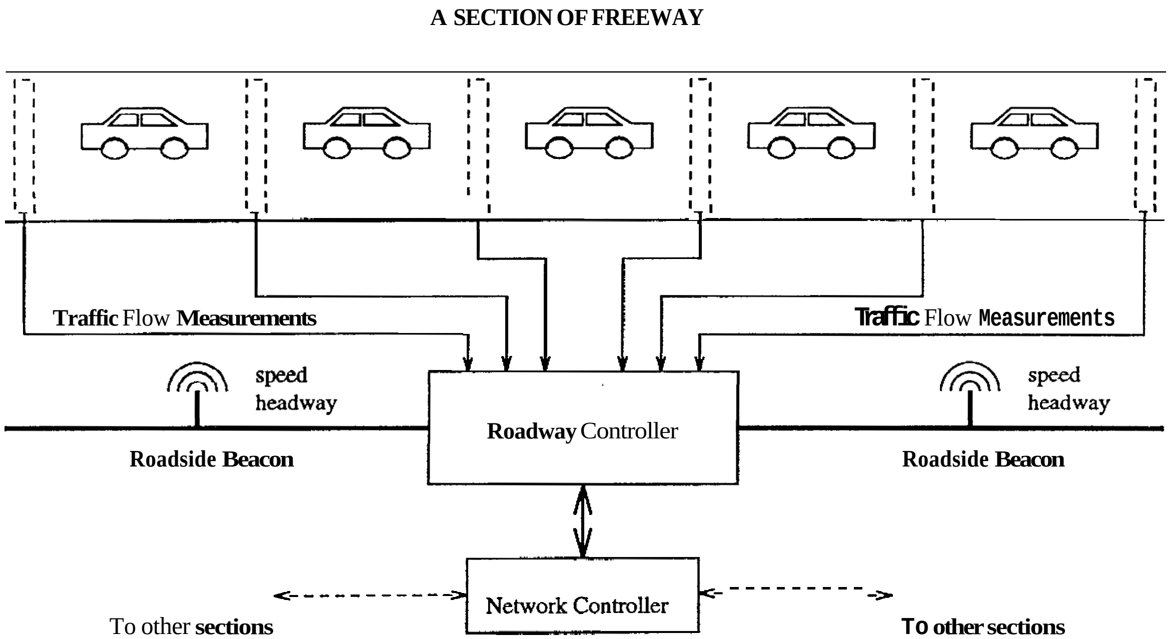

Figure 1: An AHS configuration.

A general AHS configuration that captures a wide class of AHS concepts is shown in Figure 1, where the infrastructure may issue speed and headway commands to the vehicles, in an effort to produce uniform and homogeneous traffic flow conditions, which in turn can guarantee stable and higher traffic flows [12]. In this configuration a distributed control is exercised, where the control loop contains part of the infrastructure as well as the vehicle itself. In terms of the classification defined in [13], the complete control hierarchical structure is shown in Figure 2. The structure is defined in terms of different layers,,the network and link layer lies with the infrastructure, whereas the coordination, regulation and physical layers reside in the vehicle.

In terms of the structure shown in Figure 2, the infrastructure control consists of the network and link layer or roadway controller. The network controller optimizes the operation of the traffic network by issuing routing instructions, traffic synchronization commands and by providing desired traffic distributions for the various branches of the network to the link layer or roadway controllers. The roadway controller manages a branch of the network such as a large section of the highway. It receives desired traffic density distributions from the network controller, traffic flow measurements from the section and issues speed and headway commands to the vehicles in its section, in order to change the traffic density to the desired one. The speed and headway commands can be transmitted by using the road side beacons (see Figure 1) or other communication techniques.

The vehicles operating in the **AHS** configuration of Figure 1 are equipped with the appropriate control systems that allow them to respond to the roadway commands **as** well **as** to the commands of the driver (during transitions). In addition the on-board control systems have to be able to process the information received from their own sensors and depending on the mode of operation communicate and coordinate maneuvers with other vehicles.

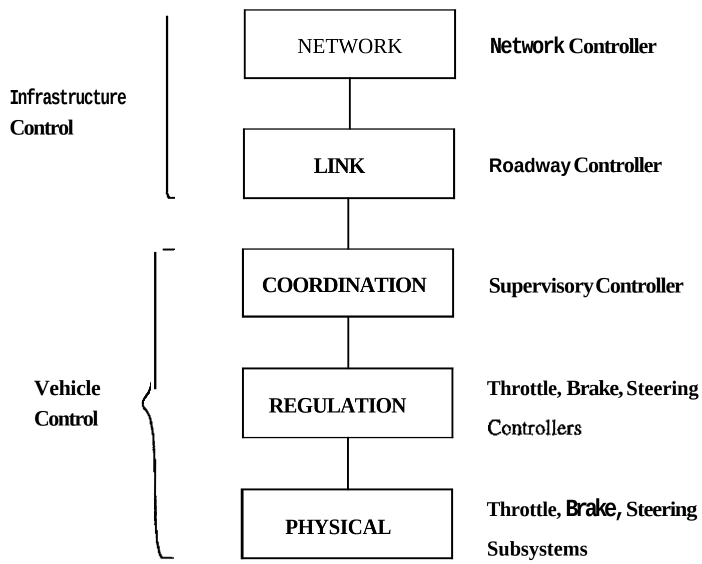

Figure 2: Distributed control structure **for** infrastructure managed vehicle control.

The on-board control system includes the coordination and regulation layers shown in Figure 2. The coordination layer consists of a supervisory controller that is responsible for self-diagnostics, recognizing the desired mode of operation, communicating with the link layer, other vehicles and the driver and issuing appropriate.commands to the regulation layer. The regulation layer consists of the throttle, brake and steering controllers that are activated by the supervisory controller and generate the appropriate commands to the actuators that reside in the physical layer.

In this paper we concentrate on the coordination layer by designing the structure of the supervisory controller for longitudinal control that may be used for several modes of vehicle following operations described in the following subsections.

2.1 Intelligent Cruise Control (ICC)

Intelligent cruise control (ICC) is a near term device that will allow automatic vehicle following under the possible supervision of the driver. In this case the driver sets the desired speed and headway and passes the task of vehicle following to the ICC system. The driver is responsible for steering and for recognizing and responding *to* emergencies. The roadway in this case may issue desired speeds to the driver using road signs etc.

The supervisory controller accepts and responds to the driver inputs, it monitors its on-board sensors, performs diagnostics and sends the appropriate commands to the throttle and brake controllers.

2.2 Cooperative Driving (no v-v communication)

In this mode of operation, the roadway to vehicle communication capability is added to the ICC system. The roadway controller can now send speed commands to the supervisory controller directly in order to control the traffic density along the highway lanes. The driver's role and responsibility remains the same as in the ICC mode, except that he/she is not allowed to set the desired speed.

With this mode of operation the supervisory controller should be able to communicate and respond to the roadway commands in addition to responding to the inputs associated with the ICC mode.

2.3 Cooperative Driving (with v-v communication)

The addition of vehicle to vehicle (v-v) communication capability allows the vehicles to communicate with the neighboring vehicles in order to negotiate and coordinate maneuvers, inform vehicles about braking capabilities, acceleration, deceleration maneuvers etc. This extra capability can be fully exploited if the ICC system is upgraded to detect and handle emergencies in the longitudinal direction. Since the control system becomes responsible for emergencies, the headway is no longer selected by the driver but is chosen by the on-board control system.

For this mode of operation the supervisory controller should be able to handle and interpret the communications with other vehicles, detect and handle emergencies in the longitudinal direction in addition to the tasks associated with cooperative driving without v-v communications. One of the important tasks of the supervisory controller is to process all the available inputs and information and select the appropriate headway in order to guarantee collision free vehicle following. In addition, the task of transition from automatic to manual is handled in a way that does not put the driver in a situation he/she cannot safely handle.

2.4 Platooning

When the vehicles are capable of communicating with each other and the roadway in addition to being able to follow each other in the longitudinal direction, it may make sense to organize them in a way that improves capacity without affecting safety. It has been proposed in [13] that the organization of vehicles in platoons of 10 to 20 with small intra-platoon but larger inter-platoon spacing (see Figure 3) will increase capacity considerably. The organization of vehicles in platoons allows the roadway to treat each platoon as a single entity and therefore eases the requirements on the bandwidth of roadway to vehicle communication system. Therefore, instead of communicating with each vehicle independently, it communicates with the leader of each platoon. The platoon leader in turn communicates with its vehicles in order to make sure the whole platoon operates as required according to the roadway commands and the traffic conditions. Since each vehicle could become a leader the supervisory controller should be designed to handle the case where the vehicle is a follower and a member of platoon as well as the case where the vehicle is a platoon leader.

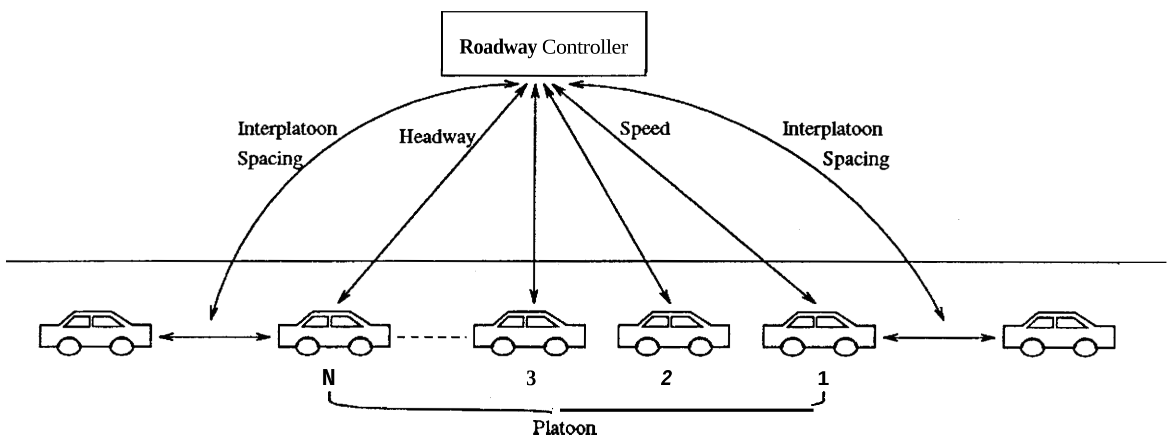

Figure 3: Platooning of vehicles as one possible mode of operation of AHS.

The reasons for considering different modes of operation are the following:

1. The vehicle should be able to operate on non-AHS facilities. Since the ICC system is developed independent of AHS, the AHS vehicle should be able to operate as any other vehicle equipped with ICC on non-AHS facilities.
2. During certain failures or traffic conditions platooning may not be the most appropriate mode of operation and the system may have to operate in the cooperative driving or even ICC mode.

3 Vehicle Longitudinal Control Design

The block diagram of the Vehicle Longitudinal Control System (VLCS) is shown in Figure 4. The supervisory controller accepts inputs from the roadway, driver, other vehicles and its on-board sensors. It processes these inputs and performs some or all of the following tasks:

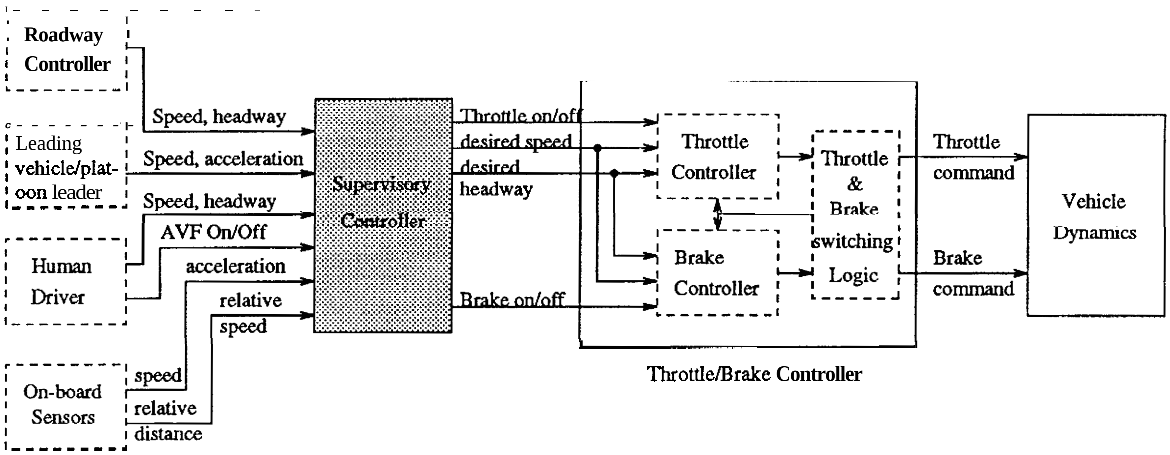

Figure 4: Vehicle longitudinal control system.

1) Determines the current mode of operation, i.e., ICC, cooperative driving, platooning etc.
2) Performs the transition operation, from manual to automatic and back to manual.
3) Selects the desired headway and speed for normal operating conditions.
4) Detects and handles emergency situations in cooperative driving and platooning.

The design objective of the supervisory controller is to smoothly execute these tasks without risking the safety and comfort of the occupants. The details of these tasks are given in the following subsections. A detailed block diagram,of the proposed supervisory controller is shown in Figure 5.

3.1 Selection of AHS Mode

The different modes of operation of AHS are classified in terms of distribution of authority between the driver and external agents, such as infrastructure, platoon leader and surrounding vehicles. Since the vehicle will be using some means to communicate with the roadway and other vehicles, it is safe to assume that these signals will be tagged or labeled to identify the source of information. Hence the logical way for determining the mode of operation of AHS is to detect the presence or absence of certain input signals.

In case no speed and headway commands are received from the roadway or platoon leader and no communication is established from the leading vehicle, ICC mode is selected. In case speed commands are received from the roadway only and no communication is detected from the platoon leader/leading vehicle, cooperative mode with no v-v communication is selected. Similarly other operating modes are selected based on the presence of

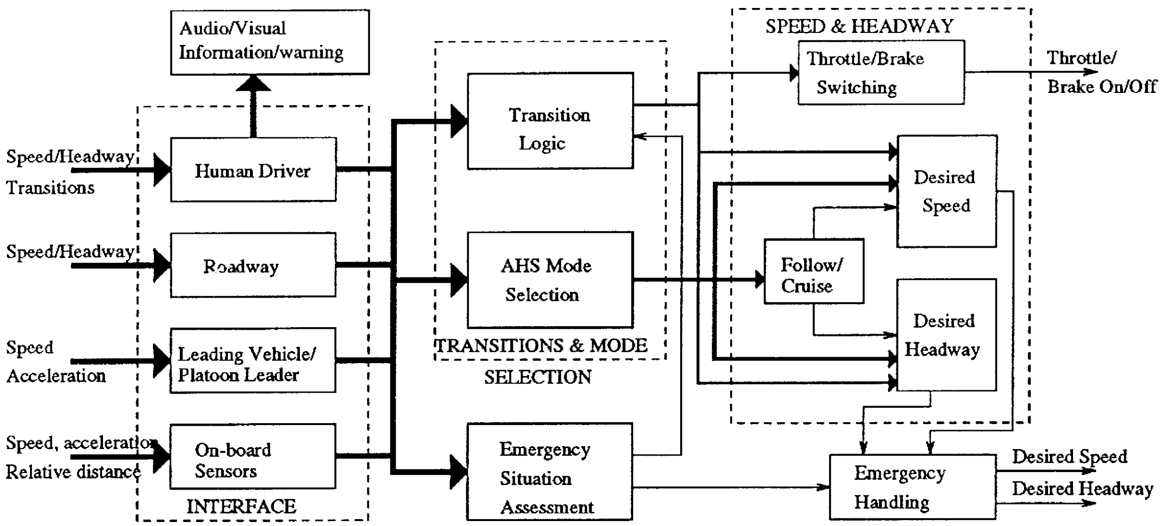

Figure 5: Detailed structure of the supervisory controller.

necessary commands from the external agents discussed in the previous section.

3.2 Transitions

The driver initiates the transition by giving the "automatic vehicle following (AVF) on" or "AVF off" input to the driver interface module of the supervisory controller. The driver interface module assigns a value to the signal $\mathcal{B}_{D_{on}}(.)$ to be used by the transition logic as shown by the flowchart in Figure 6.

The transition module uses two logical signals $\mathcal{B}_{D_{on}}(.)$, $\mathcal{B}_S(.)$ and on-board sensor readings to decide if the requested transition operation is safe to execute. For transition from manual to automatic, the driver select's the "AVF on" command that assigns a value of 1 to the signal $\mathcal{B}_{D_{on}}$. The transition module then checks the working status of all subsystems and assigns the value $\mathcal{B}_S = 1$ if the system is free of faults, otherwise $\mathcal{B}_S = 0$ is assigned. The checking of operating status of the system is a continuous process of self diagnostics using sensor measurements and fault detection algorithms, hence the automatic mode is transitioned to manual at any time a serious fault is detected.

At the end of trip, the driver initiates the automatic to manual transition process by giving "AVF off" command. This switching process involves the steps that are taken to make the driving conditions suitable for human capabilities. This is achieved by slowing down the vehicle and increasing the headway, so that the driver can easily drive the vehicle off the auto lane. The output of transition logic, $\mathcal{B}_{A_{on}}$, which shows the status of AVF, is

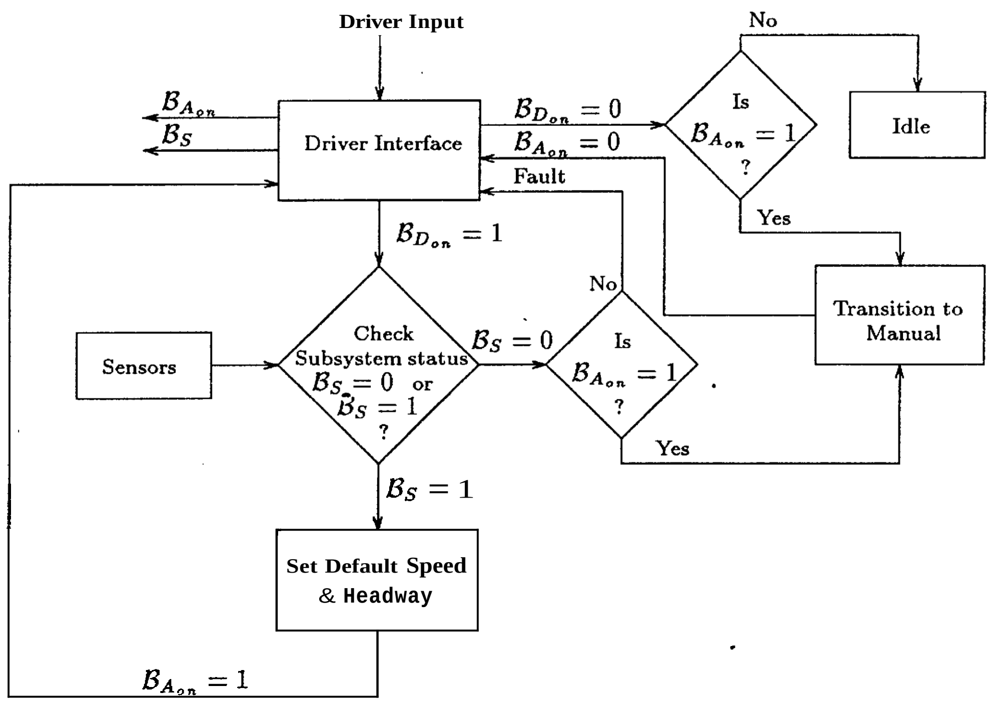

Figure 6: Logic for transitions.

a logical signal having values $\{1, 0\}$ and is given as:

$$\mathcal{B}_{A_{on}}(k) = \begin{cases} 1 & \text{if } \mathcal{B}_{D_{on}}(k) = 1 \text{ and } \mathcal{B}_S(k) = 1 \\ 0 & \text{if } (\mathcal{B}_{D_{on}}(k) = 0 \text{ or } \mathcal{B}_S(k) = 0) \text{ and } (h(k) \geq h_{max} \text{ and } V(k) \leq V_{max}) \end{cases}, \quad (2)$$

where V, h are the vehicle speed and headway respectively, V_{max} and h_{max} are the design constants and k represents the sampling instant. As given in (2) the current speed and headway are checked against certain thresholds, speed and headway are progressively increased by speed and headway selection logic till they reach the required limits. It should be noted that the process of transition from manual to automatic is the same for all modes of AHS, however, the transition back to manual mode may be different for each mode. Such as the thresholds V_{max}, h_{max} will be different for ICC than the cooperative driving and platooning. The requirement of making the driving conditions suitable for human drivers is more strict in modes of AHS where the driver is not responsible for emergency handling, such as cooperative driving with v-v communication and platooning.

3.3 Automatic Vehicle Operation

After AVF is switched on, i.e., when the transition logic has the output $\mathcal{B}_{A_{on}} = 1$, the supervisory controller proceeds with the selection of the mode of automatic vehicle operation. Two different modes of automatic vehicle operation are possible and are determined by the presence or the absence of a valid target. If there is a vehicle or obstacle, referred to as target, within the designated sensing range then the supervisory controller will choose the follow mode and if there is no target the controller will choose the cruise mode as shown in Figure 7.

The conditions for a valid target are the following:

(i) The target is within a designated range that is chosen a priori based on safety considerations.
(ii) The speed of the target is less than the speed selected by the driver (in ICC mode), or the roadway/platoon leader commanded speed (in cooperative driving/platooning mode).

If either of these two conditions is violated, the vehicle in front is not considered to be a valid target to follow. The conditions given above can be combined to form a "follow target" condition $\mathcal{B}_F(.)$ as:

$$\mathcal{B}_F(k) = \begin{cases} 1 & \text{if } \mathcal{B}_{A_{on}}(k) = 1 \text{ and } [\{h(k) < h_t \text{ and } (V_l(k) < V_C(k) + \Delta_1)\} \text{ or} \\ & \{(V_l(k) < V_C(k) + \Delta_2) \text{ and } \mathcal{B}_F(k-1) = 1\}] \\ 0 & \text{else,} \end{cases} \quad (3)$$

where h_t is the threshold for headway calculated from the sensing range, V_l is the speed of the leading vehicle, V_C is the roadway or driver commanded speed and Δ_1, $\Delta_2 > 0$ are

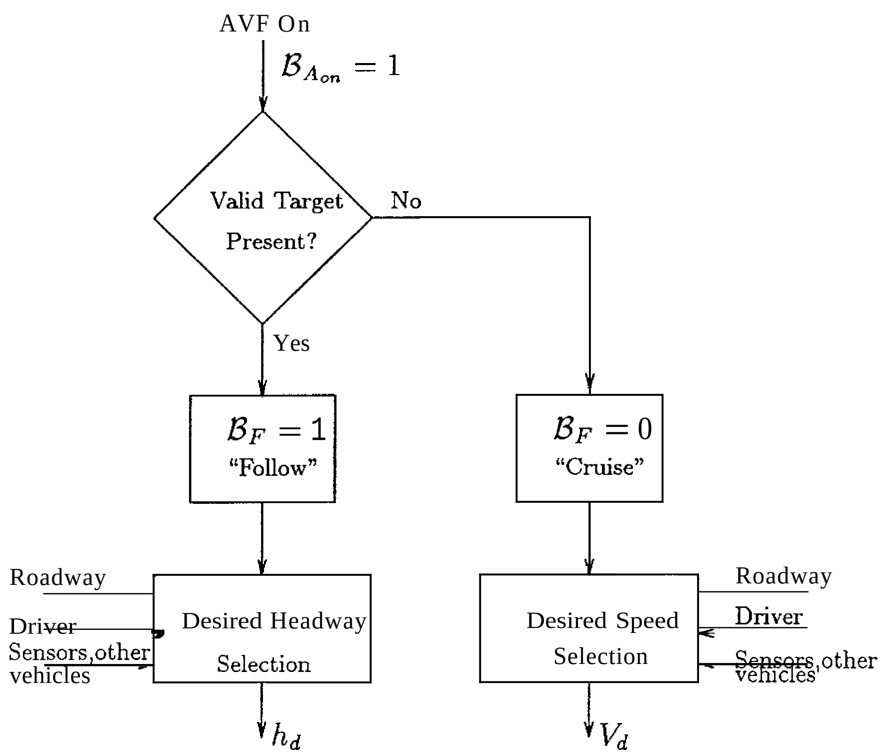

Figure 7: Operating mode selection logic.

design constants. .In **(3)** $\Delta_2 > \Delta_1$ .is used to avoid the unnecessary switching of the targets caused by the transients and/or sensor noise, hence if the target **was** previously being followed, then a larger fluctuation in target speed is tolerated. The design constants Δ_1, Δ_2 may be different for different modes of **AHS,** similarly the commanded speed V_C is different for each mode, e.g., V_C is the speed commanded by the driver in ICC mode and so on.

As shown in Figure 7, if the vehicle is in follow mode the supervisory controller has to select *a* safe headway. The calculation of the safe headway is done by the headway selection logic, which uses the inputs from the driver, roadway and other vehicles for different modes of AHS. In the follow mode the desired speed is the speed of the leading vehicle. Similarly if the vehicle is cruising, the safe cruising speed is calculated by the speed selection logic. The process of safe headway and speed selection is explained in the following subsections.

3.4 Desired Headway Selection

After AVF is switched on and the vehicle is operating in the follow mode, the desired headway selection logic has to initialize the system with a safe headway. This initializing value is taken to be the same **as** the actual headway $h(.)$, irrespective of the mode of operation of AHS. After this initialization sequence, the headway selection logic allows the driver or the external agents to change the desired headway as long as this change does not risk the safety of the system. A logical structure of this selection process in shown in Figure 8. The switching logic shown in Figure 8 contains all of the decision making process for desired headway calculation. It generates the desired headway h_i as a nonlinear function of its inputs. A filter $D(z)$ is used to generate the filtered version of the desired headway h_d. The details of different tasks performed by the headway selection module are given below. These tasks are different for each mode of operation of **AHS** and will be defined separately.

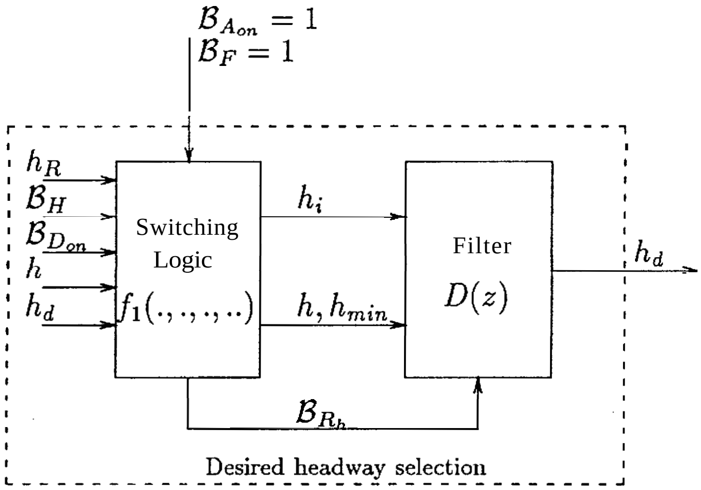

Figure 8: Block diagram of the desired headway calculation.

ICC and Cooperative Driving without v-v Communication

The state diagram of switching logic for this case is shown in Figure **9. A** "headway reset" operation is performed during initialization or whenever the "follow" mode is switched on. During this the value of $h_d(.)$ is chosen to be the current headway $h(.)$ as long as it is greater than the minimum allowable headway h_{min}. This task is performed irrespective of the mode of operation of **AHS** and ensures that there are no large transients, even though the conditions at switching are not close to the desired ones. Hence the value of $h_d(.)$ during reset operation is:

$$h_d(k) = \max(h(k), h_{min}) \quad \text{if} \quad \mathcal{B}_{R_h}(k) = 1, \tag{4}$$

where $\mathcal{B}_{R_h}(.)$ is the condition used to trigger the headway reset operation. As pointed out before that a resetting operation is performed by the switching logic whenever the AVF is switched on or a valid target appears in the cruise mode. The reset headway command

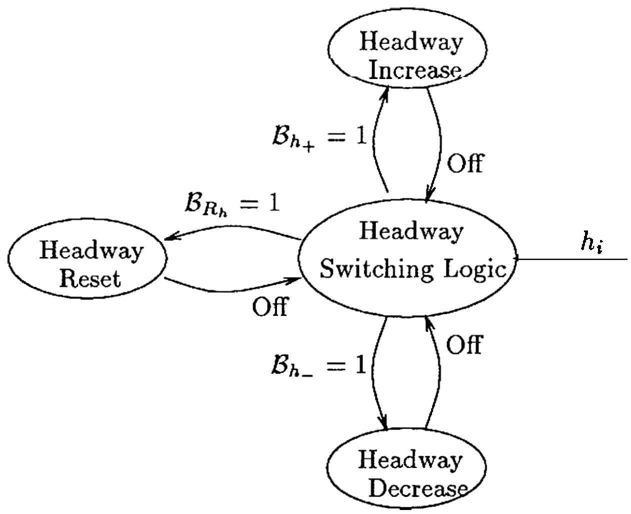

Figure 9: State diagram for headway switching logic.

$\mathcal{B}_{R_h}(.)$ is calculated **as:**

$$\mathcal{B}_{R_h}(k) = \begin{cases} 1 & \text{if } (\mathcal{B}_{A_{on}}(k) = 1 \text{ and } \mathcal{B}_{A_{on}}(k-1) \neq 1) \text{ or } (\mathcal{B}_F(k) = 1 \text{ and } \mathcal{B}_F(k-1) \neq 1) \\ 0 & \text{else.} \end{cases} \quad (5)$$

Since in ICC and cooperative driving without v-v communication, the driver is allowed to adjust the headway according to his/her comfort level, the requests for headway changes are processed by using the "headway increase" and "headway decrease" operations shown in Figure 9. The headway is increased/decreased by a predefined step size Δh and this change is accomplished through the output signal, $h_i(.)$ from the switching logic given below:

$$h_i(k) = \begin{cases} \Delta h & \text{if } \mathcal{B}_{h_+}(k) = 1 \\ -\Delta h & \text{if } \mathcal{B}_{h_-}(k) = 1 \\ 0 & \text{else,} \end{cases} \quad (6)$$

where, $\mathcal{B}_{h_+}(.)$, $\mathcal{B}_{h_-}(.)$ are the conditions for starting the headway increase and headway decrease operations respectively. The headway decrease operation is triggered only after detecting a headway decrease command from the driver. On the other hand, headway increase operation can also be started by "transition to manual" operation. As shown in Figure 6, a transition to manual operation is performed whenever the driver wants to switch off the AVF or a fault is detected in any critical subsystem. However, **as** given in (2), the transition operation requires that the headway be greater than certain threshold h_{max} and the speed less than V_{max}. All **of** these conditions are formulated in the form of logical signals

$\mathcal{B}_{h_+}(.)$ and $\mathcal{B}_{h_-}(.)$ given below:

$$\mathcal{B}_{h_+}(k) = \begin{cases} 1 & \text{if } (\mathcal{B}_F(k) = 1 \text{ and } \mathcal{B}_H(k) = 0) \text{ or } \mathcal{B}_{A_{off}}(k) = 1 \\ 0 & \text{else} \end{cases} \tag{7}$$

$$\mathcal{B}_{h_-}(k) = \begin{cases} 1 & \text{if } \mathcal{B}_F(k) = 1 \text{ and } \mathcal{B}_H(k) = 1 \text{ and } \mathcal{B}_{A_{off}}(k) = 0 \\ 0 & \text{else,} \end{cases} \tag{8}$$

where $\mathcal{B}_H(.)$, $\mathcal{B}_{A_{off}}(.)$ are the conditions for processing the headway commands from the driver and transition to manual operation respectively. The condition used by the switching logic to process the headway commands form the driver, $\mathcal{B}_H(.)$, ensures that $h \in [h_{min}, h_{max}]$ and is given below:

$$\mathcal{B}_H(k) = \begin{cases} 0 & \text{if } \mathcal{B}_{D_h}(k) = 0 \text{ and } h(k) < h_{max} \text{ and } h_d(k-1) < h^d_{max} \\ 1 & \text{if } \mathcal{B}_{D_h}(k) = 1 \text{ and } h(k) > h_{min} \text{ and } h_d(k-1) > h_{min}, \end{cases} \tag{9}$$

where h^d_{max} is a design constant and $\mathcal{B}_{D_h}(.)$ is an output signal from the driver interface to process the headway changes requested by the driver, $\mathcal{B}_{D_h} = 0$ when the driver wants to increase the headway and $\mathcal{B}_{D_h} = 1$ otherwise. **As** pointed out before that the signal $\mathcal{B}_{A_{off}}(.)$ tests the conditions at the time of transition to manual mode and is given **as:**

$$\mathcal{B}_{A_{off}}(k) = \begin{cases} 1 & \text{if } \{\mathcal{B}_{A_{on}}(k) = 1 \text{ and } (\mathcal{B}_{D_{on}}(k) = 0 \text{ or } \mathcal{B}_S(k) = 0) \text{ and } (h(k) < h_{max} \\ & \quad \text{or } V(k) > V_{max}) \text{ and } h_d(k-1) < h^d_{max}\} \\ 0 & \text{else.} \end{cases} \tag{10}$$

As shown in Figure 8, the headway command generated by the switching logic $h_i(.)$ is filtered to avoid excessive transients. The filtered desired headway command h_d is given **as:**

$$h_d(k) = h_d(k-1) + Th_i(k), \tag{11}$$

where T is the sampling time and $h_i(.)$ is given in (6).

Cooperative Driving with v-v Communication and Platooning

The state diagram of switching logic for this case is shown in Figure 10. **As** pointed out before that the "headway reset" task is same for each mode of operation of AHS, hence the relations in this case are the same **as** given in (4) and *(5).* However, the design constant h_{min} may be different for each mode of AHS.

In ICC and cooperative driving mode without v-v communication, the actual headway h is taken **as** the desired headway command from the driver, with the assumption that the driver will switch on the AVF when the vehicle is following the preceding vehicle at **a**

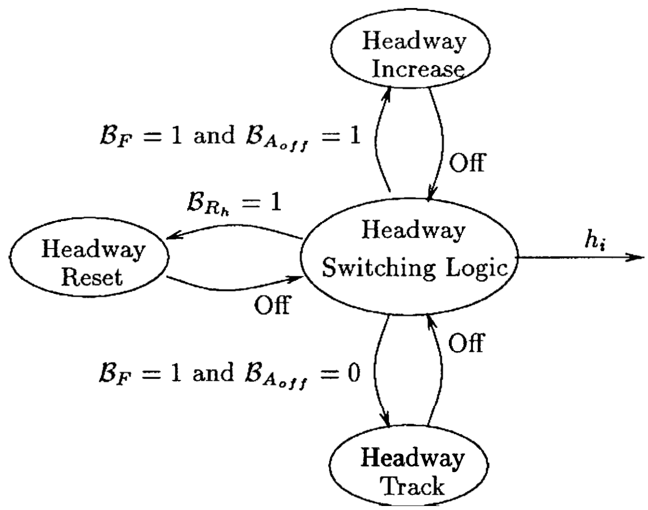

Figure 10: State diagram for headway switching logic.

comfortable distance. However, in cooperative driving with v-v communication and platooning modes the headway h at the time of resetting can be different than the roadway commanded headway h_R, (in the case of platooning h_R is received indirectly through the platoon leader). The desired headway in this case is smoothly changed to h_R by using the "headway **track"** operation shown in Figure 10. **Also** shown in Figure 10 is the "headway increase'' task, which is performed only when the transition to manual mode is required. The output of the switching logic $h_i(.)$ in this case is:

$$h_i(k) = \begin{cases} k_p(h_R(k) - h_d(k-1)) & \text{if } \mathcal{B}_F(k) = 1 \text{ and } \mathcal{B}_{A_{off}}(k) = 0 \\ \Delta h & \text{if } \mathcal{B}_F(k) = 1 \text{ and } \mathcal{B}_{A_{off}}(k) = 1 \\ 0 & \text{else,} \end{cases} \quad (12)$$

where k_p is a design constant and $\mathcal{B}_{A_{off}}(.)$ is the same **as** given in (10). In (12) it is assumed that, $h_R \in [h_{min}, h_{max}]$. Again the filter $D(z)$ .given in **(11)** is used in this case too. For reference a complete expression for the desired headway command $h_d(.)$ is given below:

$$h_d(k) = \begin{cases} \max(h(k), h_{min}) & \text{if } \mathcal{B}_{R_h}(k) = 1 \\ h_d(k-1) + T h_i(k) & \text{else,} \end{cases} \quad (13)$$

where $h_i(.)$ is given by either **(6)** or (12) depending on the mode of operation of **AHS.**

3.5 Desired Speed Selection

If the vehicle is operating in the cruise mode, the speed selection logic calculates a desired speed to be given to the throttle/brake controller. If the vehicle is operating in ICC the desired speed is selected by the driver while in cruise mode. In this case the vehicle is traveling without any valid target in front. In the case of cooperative driving and platooning, desired speed is issued by the roadway. While platooning the vehicle can be in the cruise mode only if it is a platoon leader. The structure of the desired speed selection logic is the same as that of the desired headway, shown in Figure 8. The functions performed by the switching logic in this case are given below.

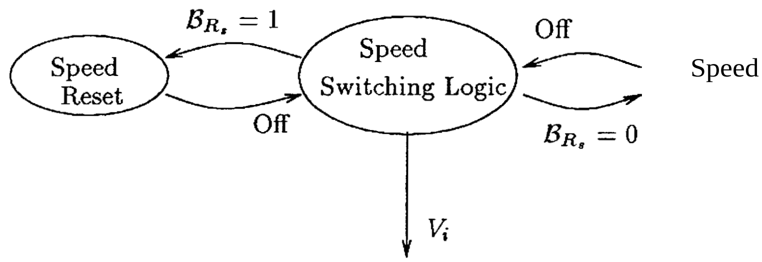

Figure 11: State diagram for the speed switching logic.

The state diagram for speed switching logic is shown in Figure 11. For the desired speed selection we are assuming a different kind of driver interface in which the speed command from the driver is available in exact numbers instead of increase/decrease command considered for headway selection. Hence the state diagram shown in Figure 11 is same for each mode of AHS, the only difference is that the speed command for "speed track" operation has different sources.

A "speed reset" operation is performed whenever the AVF is switched on and the desired speed V_d is taken as the current speed of the vehicle V. This resetting condition avoids large speed transients at the time when the AVF is switched on. Hence

$$V_d(k) = V(k) \quad \text{if} \quad \mathcal{B}_{R_s}(k) = 1, \tag{14}$$

where, $\mathcal{B}_{R_s}(.)$ is the speed reset command and is generated as:

$$\mathcal{B}_{R_s}(k) = \begin{cases} 1 & \text{if } \mathcal{B}_{A_{on}}(k) = 1 \text{ and } \mathcal{B}_{A_{on}}(k-1) \neq 1 \\ 0 & \text{else.} \end{cases} \tag{15}$$

After initialization, the desired speed V_d is made to track the speed command V_C through "speed track" operation. The speed switching logic generates a signal $V_i(.)$ which is passed through a filter $D_1(z)$ designed with comfort constraints. The speed command V_i generated by the switching logic is given as:

$$V_i(k) = \begin{cases} k_i Sat_1(r(k-1) - V_d(k-1)) & \text{if } \mathcal{B}_{A_{off}}(k) = 1 \\ k_i Sat_2(r(k-1) - V_d(k-1)) & \text{else,} \end{cases} \tag{16}$$

where, k_i is a design constant, $Sat_1(.)$, $Sat_2(.)$ are saturation functions and $\mathcal{B}_{A_{off}}(.)$ is the same as given in (10), which is used to determine if the speed and headway at the time of transition to manual mode are within the specified limits. In (16), $r(.)$ is given as:

$$r(k) = \begin{cases} V_s & \text{if } \mathcal{B}_{A_{off}}(k) = 1 \\ s(k) & \text{else,} \end{cases} \tag{17}$$

where, $V_s > 0$ is a design constant and is the vehicle speed when the control is finally transferred to the driver after transition, usually taken to be equal to the nominal highway speed. The signal $s(.)$ in (17) chooses the source of desired speed command for different modes of AHS and is given as:

$$s(k) = \begin{cases} V_l(k) & \text{if } \mathcal{B}_F(k) = 1 \\ V_C(k) & \text{else,} \end{cases} \tag{18}$$

where V_l is the speed of the leading vehicle and V_C is the speed command provided by the driver or infrastructure. As discussed before, in ICC mode V_C is issued by the driver, whereas in cooperative driving and platooning $V_C = V_R$. However, in platooning mode, only the platoon leader can operate in the cruise mode and hence can receive speed commands from the roadway. The rest of the platoon takes the desired speed and headway commands through the platoon leader. It will be shown later in the simulation section that the conditions for following a target given in (3) and switching the desired speed from the leader speed to the roadway speed, as given in (18), prevents excessive overshoot when the platoon executes a slowing down maneuver. The speed command $V_i(.)$ is passed through a filter $D_1(z)$ which is given as:

$$V_d(k) = V_d(k-1) + TV_i(k). \tag{19}$$

It should be noted that $(r(k-1) - V_d(k-1))$in (16) at the input of the integrator (19) is an acceleration term. Therefore the comfort constraints imposed in terms of maximum allowable acceleration and deceleration are given in (16) as saturation functions, $Sat_1(.)$ and $Sat_2(.)$, where

$$Sat_1(r - V_d) = \begin{cases} A_{max} & \text{if } (r - V_d) \geq A_{max} \\ A_{min} & \text{if } (r - V_d) \leq A_{min} \\ r - V_d & \text{else} \end{cases} \tag{20}$$

$$Sat_2(r - V_d) = \begin{cases} A'_{max} & \text{if } (r - V_d) \geq A'_{max} \\ A'_{min} & \text{if } (r - V_d) \leq A'_{min} \\ r - V_d & \text{else} \end{cases} \tag{21}$$

where A_{max}, $A'_{max} > 0$ and $A_{min}, A'_{min} < 0$ are design constants. The limits for maximum allowable acceleration and deceleration are different during transition to manual mode, which is obvious from (20) and (21), where $A_{max} \leq A'_{max}$ and $A_{min} \geq A'_{min}$. For reference, a complete expression for the desired speed command $V_d(.)$ is give below:

$$V_d(k) = \begin{cases} V_d(k-1) + TV_i(k) & \text{if } \mathcal{B}_{R_s}(k) = 0 \\ V(k) & \text{else.} \end{cases} \tag{22}$$

3.6 Emergency Operation

In cooperative driving and platooning modes, the recognition and handling of emergencies is one of the tasks performed by the supervisory controller. The recognition of emergencies requires that the input signals be continuously monitored for detecting the presence of any abnormal pattern or behavior. Once an emergency situation is detected, a set of actions is performed by an emergency handling logic. The recognition and handling of emergencies is discussed in subsections below.

3.6.1 Emergency Situation Assessment

The presence of a potential emergency situation is estimated by detecting an unusual pattern in the input signals. The common kind of emergencies encountered while driving in the automatic following mode are:

1) subsystem failure,
2) potentially dangerous target in cruise/follow mode.

For detecting subsystem failure, the assessment logic receives operating status of all the major subsystems of the vehicle. In case a failure is detected in any critical subsystem by the failure detection logic, an emergency situation is declared to be present.

The presence of a potentially dangerous target while operating in the cruise or follow mode can be determined by comparing the measured time to collision (TTC) against a minimum time for stopping the vehicle safely. At any time t, the relative distance X_r between the vehicles can be written as:

$$X_r(t) = X_r(t_0) + [V_l(t_0) - V_f(t_0)](t - t_0) + \int_{t_0}^{t}\int_{t_0}^{\tau}[a_l(s) - a_f(s)]ds\, d\tau, \tag{23}$$

where, V_l and V_f are the speeds of leading and following vehicles respectively, a_l and a_f are the accelerations of leading and following vehicle respectively and t_0 is the time at which the measurement of TTC is required. If for some time $t > t_0$ $X_r(t) = 0$, then TTC $=$ $t - t_0$. Since the calculation of TTC requires prediction of the deceleration profiles for the leading and following vehicle for the time interval $[t_0, t]$, different assumptions can be made to approximate its value. For a rough cut estimate of TTC, we can assume that $a_f(\tau) = a_l(\tau)$ $\forall \tau \in [t_0, t]$. Also with the assumption that the ranging sensor provides both the relative distance and speed information, the TTC can be calculated **as:**

$$TTC = \frac{\mathbf{AX}}{\mathrm{AV}} \tag{24}$$

where A X $= X_r(t_0)$ and AV $= V_f(t_0) - V_l(t_0)$ are the measured relative distance and speed respectively **at** time to. For TTC to have any significance it is required that AV > 0. For a more conservative estimate of TTC, we can assume that the leading vehicle is decelerating with the maximum possible deceleration allowed in emergency condition and the trailing vehicle is braking with maximum deceleration allowed in the automatic following mode, i.e., $a_l(\tau) = a_{l_{min}}$, $a_f(\tau) = a_{min}$ $\forall \tau \in [to,t]$,then:

$$(a_{l_{min}} - a_{min})(t - t_0)^2 - \Delta V(t - to) + \mathbf{AX} = 0, \tag{25}$$

where a_{min} is the maximum deceleration allowed in the automatic following mode and $a_{l_{min}}$ is the maximum possible deceleration of the leading vehicle. From (25), TTC can be written **as:**

$$TTC = \frac{-\mathbf{AV} + \sqrt{\Delta V^2 + 4\Delta X \Delta a}}{2\Delta a}, \tag{26}$$

where, $Aa = a_{min} - a_{l_{min}} > 0$. The actual value of TTC lies between that given in (24) and (26), however, from the safety point of view, we will use the more conservative estimate given in (26).

The calculation of the minimum stopping time of the vehicle, t_{min}, however, involves some of the most un-deterministic parameters of the vehicle, i.e., the surface friction coefficient and the effective braking force on the wheels. However, with the assumption of a fairly constant braking capabilities, we can use different scenarios explored in [1] to estimate the minimum stopping time.

To calculate t_{min}, we use the scenario shown in Figure 12. After time delay t_d, which, includes processing and actuator delays, the brakes are applied with the maximum jerk J_{max}, $(t_b - t_d)$ is the time it takes to reach the maximum deceleration a'_{min}, then:

$$t_d = T_1 + \tau, \tag{27}$$

$$t_b = \frac{a'_{min}}{J_{max}} + t_d, \tag{28}$$

where T_1 and τ are the processing and actuator delays respectively. The value of t_{min} is calculated by using the condition given below:

$$V(t_d) + \int_{t_d}^{t_{min}} a(t)dt = 0. \tag{29}$$

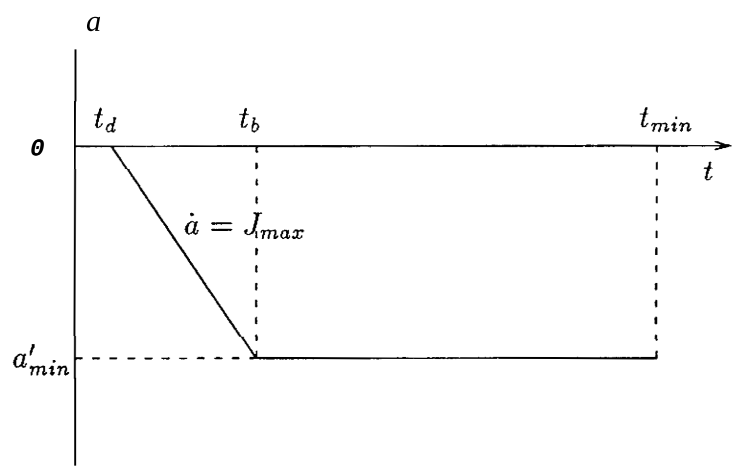

Figure 12: Scenario for calculation of minimum stopping time.

Hence,

$$\begin{aligned} & V(t_d) - \frac{1}{2}J_{max}(t_b - t_d)^2 - a'_{min}(t_{min} - t_b) = 0, \\ \Rightarrow \; & t_{min} = \frac{V(t_d) - \frac{1}{2}J_{max}(t_b - t_d)^2}{a'_{min}} + t_b, \end{aligned} \tag{30}$$

where $a(.)$ is the acceleration and $V(.)$ is the speed of the vehicle.

However, since the comparison of TTC with the stopping time require measurements from the sensors and calculations, it introduces a certain amount of delay, which in some cases may prove to be the bottleneck of the emergency situation.handling scheme. That is the reason for requiring v-v communication for detection of emergency situation. Since with the existence of v-v communication, presence of emergency in most cases can be estimated. without significant delay by receiving the acceleration/deceleration commands from the preceding vehicle. Hence the triggering point for the detection of an emergency situation is that the deceleration of the leading vehicle a_l is more than a threshold, i.e.,

$$\text{if } a_l < a_{min} \Rightarrow \text{emergency exists,}$$

where, $a_{min} < 0$ is the maximum deceleration allowed in the normal automatic following mode. Hence the presence of emergency is estimated as:

$$\mathcal{B}_E(k) = \begin{cases} 1 & \text{if } a_l < a_{min} \text{ or } TTC < t_{min} \\ 0 & \text{else.} \end{cases} \tag{31}$$

3.6.2 Emergency Situation Handling

Two major functions performed by the supervisory controller are the desired speed and headway calculation, hence are affected by the presence of an emergency situation. The desired values given earlier are modified to take into account the prevailing emergency situation.

The set of actions taken to handle subsystem failures depends on the level of redundancy provided in the system design. If redundancy is available for all critical subsystems, such as throttle, brake, steering actuators and sensors, then in the case of failure a warning is issued and AVF is switched off. This transition procedure is completed with the help of redundant sensors or actuators. As discussed before, the desired speed and headway selection logics use the signal $\mathcal{B}_{A_{off}}(.)$ in (10) to detect if the driver wants to switch to manual mode or if there is any failure in the system. In the case of failure $\mathcal{B}_{A_{off}} = 1$, then as given in (6), (12) and (17) the desired headway is increased and the desired speed is decreased till the actual headway and speed reach a safe value. However, in case no redundancy is available, the driver is instructed to complete the transition process manually and to drive the vehicle out of the auto lane.

A target can be declared potentially dangerous while the vehicle is operating in either the cruise or follow mode. The steps taken to handle the emergency situation in this case is to modify the desired speed and headway commands calculated for normal operating mode. In order to formulate the modification of the desired headway and speed commands (13), (22), we define the relative magnitude of emergency as:

$$M_E(k) \triangleq min\left[max\left\{\left(1-\frac{TTC}{t_{min}}\right),\left(\frac{a_{min}-a_l}{a_{min}-a'_{min}}\right),0\right\},1\right], \tag{32}$$

where a'_{min} is the maximum possible deceleration of the vehicle.. It should be noted that $M_E(k) \in [0,1]$. We further define the maximum change in the vehicle speed, ΔV^b_{max}, and hence the maximum change in the headway Δh^b_{max} in one sampling interval due to the .application of maximum allowable **braking** force f^b_{max}.

$$\Delta V^b_{max} \triangleq -\frac{f^b_{max}}{M}T, \tag{33}$$

$$\Delta h^b_{max} \triangleq \frac{f^b_{max}}{VM}Th, \tag{34}$$

where, M is the mass of the vehicle, V, h are the current speed and headway of the vehicle respectively. Hence the change in desired headway, Δh_d, and the desired speed, ΔV_d, can be calculated by scaling down their maximum values Δh^b_{max} and ΔV^b_{max} respectively, i.e.,

$$\Delta h_d = \Delta h^b_{max}\left[1-e^{-\frac{M_E}{1-M_E}}\right], \tag{35}$$

$$\Delta V_d = \Delta V^b_{max}\left[1-e^{-\frac{M_E}{1-M_E}}\right]. \tag{36}$$

Hence with the existence of an emergency, the calculation of the desired headway and speed can be changed as:

$$h'_d(k) = \begin{cases} h_d(k) + \Delta h_d(k) & \text{if } \mathcal{B}_E(k) = 1 \\ h_d(k) & \text{else,} \end{cases} \tag{37}$$

$$V'_d(k) = \begin{cases} V_d(k) + \Delta V_d(k) & \text{if } \mathcal{B}_E(k) = 1 \\ V_d(k) & \text{else.} \end{cases} \tag{38}$$

The simulation results for an emergency situation in which the leading vehicle slows down with a constant deceleration of 0.3g is shown in Figure 13.

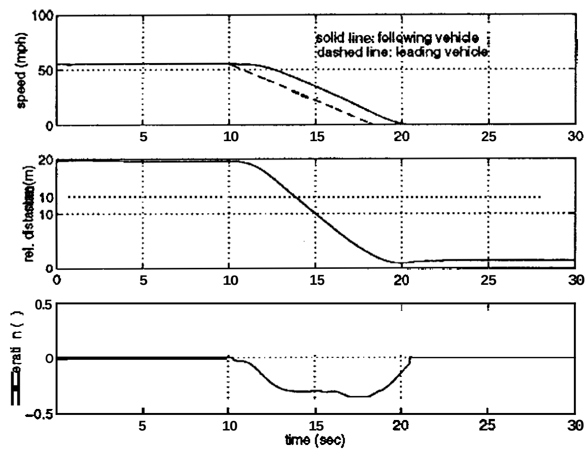

Figure 13: At $t_0 = 10$ sec the leading vehicle slows down at a constant rate of -0.3g. The following vehicle with $X_r(t_0) = 19.5$ m (.corresponding to time headway of 0.8 sec) manages to stop without collision.

4 Stability and Performance Analysis

In this section we will analyze the stability of the overall closed loop system shown in Figure 4. For analysis purpose the block diagram is redrawn in Figure 14, showing all the states and input/output for each block separately. For completeness sake we will briefly describe the vehicle dynamics model here, a complete study can be found in [10, 14, 15].

Two control inputs, the throttle angle and the braking torque, are used to control the motion of the vehicle in the longitudinal direction. The speed of the vehicle V is a nonlinear function of the throttle angle θ, i.e.,

$$V = F(\theta, t, \tau). \tag{39}$$

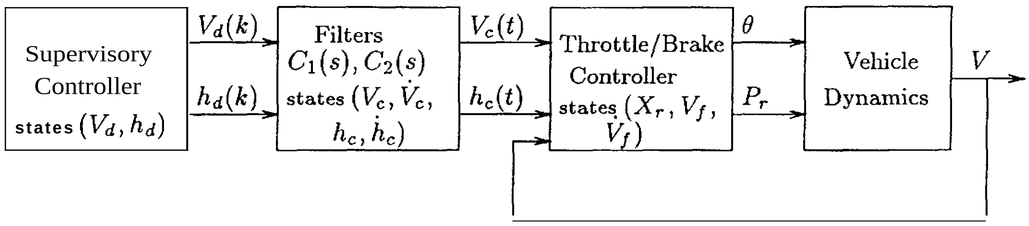

Figure **14:** Closed loop system for stability analysis.

Various expressions for the nonlinear function $F(\theta, t, \tau)$ exist in the transportation literature and can be found in [14, 15]. For normal vehicle operation, the nonlinear model **(39)** can be approximated by **a** linearized model given below:

$$\frac{\bar{V}}{\bar{\theta}} \approx \frac{\hat{b}}{s + \hat{a}}, \tag{40}$$

where, $\bar{V} = V - V_0$ and $\bar{\theta} = \theta - \theta_0$ are the deviations of (V, θ) from the operating point (V_0, θ_0) and the model coefficients, $\hat{a}$, $\hat{b}$ are function of operating point. The model (40) can be rewritten **as:**

$$V = -\hat{a}\bar{V} + \hat{b}\bar{\theta} + d, \tag{41}$$

where the disturbance term, d, accounts **for** the neglected dynamics in (40). Similarly, the dynamic equation of the braking torque to the vehicle speed is given **as:**

$$\dot{V} = \frac{1}{M}\left(-c_1 T_b - f_0 - c_2 V - c_3 V^2\right), \tag{42}$$

where T_b is the braking torque, M is the vehicle mass, f_0, c_2V, c_3V^2 represent the static friction force, rolling friction force and air resistant force respectively. The term $c_1 T_b$ in (42) is the braking force and is proportional to the brake line pressure P_r shown in Figure 14 **as** a control input. For this study we will use the nonlinear PID throttle controller and the brake controller designed with feedback linearization in [10] to represent the throttle/brake controller in Figure **14.** Since the throttle/brake controller requires continuous signals **as** the desired speed and headway, the discrete time signals $V_d(k)$ and $h_d(k)$ are filtered to generate continuous signals $V_c(t)$ and $h_c(t)$ respectively, shown in Figure **14.** For throttle controller, the dynamic equations of the vehicle following are:

$$\begin{aligned}
X_r &= V_l - V_f, \\
\dot{V}_f &= -\hat{a}(V_f - V_l) + \hat{b}\bar{\theta}_f + d, \\
\delta &= X_r - hV_f - S_0, \\
V_r &= V_l - V_f,
\end{aligned} \tag{43}$$

where δ is the deviation from the desired spacing, V_l is the speed of the leading vehicle (desired speed), V_r is the relative speed, S_0 is a constant and $\bar{\theta}_f = \theta_f - \theta_0$ is the throttle angle to be generated by the control law. For PID controller $\bar{\theta}_f$ is given **as:**

$$\bar{\theta}_f = k_1 V_r + k_2 \delta + \int_0^t (k_3 V_r + k_4 \delta) d\tau. \tag{44}$$

The gains $k_1 \ldots k_4$ are chosen to place the closed loop poles at the desired locations. In [10] it is shown that the control law **(44)** guarantees that with constant h and V_l, 6, $V_r \to 0$ (exponentially). Similarly for the brake controller the closed loop system after feedback linearization is:

$$\begin{aligned} \dot{X}_r &= V_l - V_f, \\ \dot{V}_f &= k_5 V_r + k_6 \delta, \\ \delta &= X_r - h V_f - S_0, \\ V_r &= V_l - V_f, \end{aligned} \tag{45}$$

where k_5 and k_6 are the gains to be selected to make the closed loop system stable and to guarantee that δ, $V_r \to 0$ for constant h and V_l. However, with the supervisory controller in the loop the desired speed and headway $V_c(t)$ and $h_c(t)$ cannot be assumed to be constant. Hence some analysis is required to show the closed loop stability with time varying desired speed and headway commands. In the analysis to follow, we will use the following Lemma [16].

Lemma 4.1 *If the linear system:*

$$\dot{x} = A(t)x \qquad \text{where } A \text{ is continuous } \forall t \geq t_0,$$

*is uniformly asymptotically **stable** (u.a.s.) then the system:*

$$\dot{x} = [A(t) + B(t)]x,$$

***is** also u.a.s. **if** $B(t)$ is continuous $\forall t \geq t_0$ and **if** $B(t) \to 0$ **as** $t \to \infty$.*

Using Lemma **4.1,** the following Theorem establishes the stability of the closed loop system shown in Figure **14.**

Theorem 4.1 *(i) All the signals in closed **loop** system **of** Figure 14 are bounded.*

*(ii) **if** $V_d(k) \to c_1$ and $h_d(k) \to c_2$, where c_1, $c_2 > 0$ are constants then δ, $V_r \to 0$.*

Proof: (i) The boundedness of the closed loop signals will be shown in two steps.

Step 1. As shown in Figure **14,** the supervisory controller with the filters generate the desired trajectory, hence in first step we will show that $V_c(t)$ and $h_c(t)$ are bounded. The switching logic in the speed and headway selection logic guarantees that $V_i(k) \in [V_{min}, V_{max}]$ and $h_i(k) \in [h_{min}, h_{max}]$. From (22) and **(13)** we have that $V_d(k)$, $h_d(k) \in l_\infty$. **Also** the filters $D_1(z)$ and $D(z)$ in (22), **(13)** are designed *so* that $\Delta V_d(k)$, $\Delta h_d(k) \in l_\infty$, where $\Delta f(k) = f(k) - f(k-1)$. Since $V_c(s) = C_1(s)V_d(k)$ and $h_c(s) = C_2(s)h_d(k)$ with $V_d(k)$, $h_d(k) \in l_\infty$, filters $C_1(s)$ and $C_2(s)$ can be designed such that V_c, $\dot{V}_c \in \mathcal{L}_\infty$ and h_c, $\dot{h}_c \in \mathcal{L}_\infty$.

Step 2. Before analyzing the stability of throttle/brake system, we consider the possible variations in the headway signal $h_c(t)$. Since the headway changes occur only at finite number of instants, on requests issued by the driver or roadway, the signal $h_c(t)$ is mainly constant with finite number of transitions. Without loss of generality, we can assume that one such transition occurs at t_0, then $h_c(t)$ can be represented as, $h_c(t) = h(t_0) + h_j(1 - e^{-\alpha(t-t_0)})$, where h_j is the jump in headway at time t_0 and α is a constant determined by the filter $C_2(s)$. Hence

$$h_c(t) = \bar{h}_c + h_\Delta, \tag{46}$$

where $\bar{h}_c = h(t_0) + h_j$ is constant and $h_\Delta = -h_j e^{-\alpha(t-t_0)}$. Then for $t \geq t_0$ the closed loop system (43), **(44)** becomes:

$$\begin{aligned}
\dot{X}_r &= V_c - V_f, \\
\ddot{V}_f &= -(\hat{a} + \hat{b}k_1 + \hat{b}k_2\bar{h}_c)\dot{V}_f - (\hat{b}k_2 + \hat{b}k_3 + \hat{b}k_4\bar{h}_c)V_f - (\hat{a} + \hat{b}k_1)\dot{V}_c \\
&\quad + (\hat{b}k_2 + \hat{b}k_3)V_c + \hat{b}k_4X_r - (\hat{b}k_4h_\Delta V_f + \hat{b}k_2\dot{h}_\Delta V_f + \hat{b}k_2h_\Delta\dot{V}_f), \\
\delta &= X_r - \bar{h}_cV_f - h_\Delta V_f, \\
V_r &= V_c - V_f.
\end{aligned} \tag{47}$$

The terms S_0 and d in **(43)** are constants and have no effect on the current analysis, hence are neglected in (47). The closed loop system (47) can also be written **as:**

$$\begin{aligned}
\dot{X} &= [A + D_1(t)]X + Bu, \\
Y &= [C + D_2(t)]X + Du,
\end{aligned} \tag{48}$$

where $X = [X_r, V_f, \dot{V}_f]^T$, $u = [V_c, \dot{V}_c]^T$, $Y = [\delta, V_r]^T$. The matrices A, B, C, D, $D_1(t)$ and $D_2(t)$ in (48) are given **as:**

$$A = \begin{bmatrix} 0 & -1 & 0 \\ 0 & 0 & 1 \\ \hat{b}k_4 & -\hat{b}(k_2 + k_3 + k_4\bar{h}_c) & -(\hat{a} + \hat{b}k_1 + \hat{b}k_2\bar{h}_c) \end{bmatrix}; B = \begin{bmatrix} 1 & 0 \\ 0 & 0 \\ \hat{b}(k_2 + k_3) & -(\hat{a} + \hat{b}k_1) \end{bmatrix},$$

$$C = \begin{bmatrix} 1 & -\bar{h}_c & 0 \\ 0 & -1 & 0 \end{bmatrix}; D = \begin{bmatrix} 0 & 0 \\ 1 & 0 \end{bmatrix},$$

$$D_1(t) = \begin{bmatrix} 0 & 0 & 0 \\ 0 & 0 & 0 \\ 0 & -\hat{b}(k_4h_\Delta + k_2\dot{h}_\Delta) & -\hat{b}k_2h_\Delta \end{bmatrix}; D_2(t) = \begin{bmatrix} 0 & -h_\Delta & 0 \\ 0 & 0 & 0 \end{bmatrix}.$$

It should be noted that (A, B, C, D) from (48) are the same as that for the closed loop system (43), (44) with $h = \bar{h}_c$ and $V_l = V_c$. Now consider the homogeneous part of the LTV system (48):

$$X = [A + D_1(t)]X. \tag{49}$$

Since $X = AX$ is an exponentially stable system, $D_1(t)$ is continuous $\forall t \geq t_0$ and $D_1(t) \to 0$ as $t \to \infty$, then by Lemma **4.1** we have that (49) is u.a.s. Now **(49)** is u.a.s. if and only if $\exists\ \lambda_0, \alpha_0 > 0 \ni \|\Phi(t,\tau)\| \leq \lambda_0 e^{-\alpha_0(t-\tau)}$, for $t_0 \leq \tau \leq t < \infty$, where $\Phi(.,.)$ is the state transition matrix for **(49).** Since in step **1** we have proved that $u = [V_c, \dot{V}_c]^T \in \mathcal{L}_\infty$, by solving the LTV system **(48)** for X and Y, we have that:

$$\|X\|_\infty \leq \frac{\lambda_0 a_1}{\alpha_0}\|u\|_\infty + \epsilon,$$
$$\|Y\|_\infty \leq \left(\frac{\lambda_0 a_1 a_2}{\alpha_0} + a_3\right)\|u\|_\infty + \epsilon, \tag{50}$$

where $a_1 = \|B\|_\infty$, $a_2 = \sup_t \|C + D_2(t)\|$, $a_3 = \|D\|_\infty$ and ϵ is an exponentially decaying to zero term due to $X(t_0) \neq 0$. Hence X, $Y \in \mathcal{L}_\infty$. The same analysis can be shown for the brake controller (45). Since the throttle/brake switching logic designed in [10] guarantees that the throttle and brake controller are not acting together at the same time, all the signals and states in the closed loop system in Figure 14 are bounded.

(ii) To show that $\delta, V_r \to 0$ when $V_d(k), h_d(k) \to$ constant, we will use another representation of the closed loop system. From **(43)** and **(44)** we can get the transfer function from $\dot{V}_l$ to δ and V_r as:

$$\delta = \frac{(1 - \hat{a}h - \hat{b}k_1 h)s - \hat{b}k_3 h}{\Delta(s)}\dot{V}_l,$$
$$V_r = \frac{s^2 + \hat{b}k_2 hs + \hat{b}k_4 h}{\Delta(s)}\dot{V}_l, \tag{51}$$

where $\Delta(s) = s^3 + (\hat{a} + \hat{b}k_1 + \hat{b}k_2 h)s^2 + \hat{b}(k_2 + k_3 + k_4 h)s + \hat{b}k_4$. With supervisory controller in the loop (51) becomes:

$$\dot{e} = [A_1 + D_3(t)]e + B_1\dot{V}_c,$$
$$Y = [C_1 + D_4(t)]e, \tag{52}$$

where $e \in \mathcal{R}^3$, (A_1, B_1, C_1) is a state space representation of (51) in the controller canonical form, $D_3(t)$ and $D_4(t)$ are exponentially decaying to zero disturbance matrices obtained by replacing h with $h_c(t)$ given in **(46).** Since $D_3(t)$ follows the conditions stated in Lemma 4.1, $\dot{e} = [A_1 + D_3(t)]e$ is u.a.s. Now as $V_d(k) \to c_1 \Rightarrow \dot{V}_c \to 0$, (52) is a u.a.s. system with a bounded input which goes to zero, hence $Y = [\delta, V_r]^T \to 0$. The same result can be shown for the brake controller **(45).** □

The simulation results in Figures 17-18, where the desired speed and headway commands are made to change, support the claim asserted in Theorem **4.1.** In the following subsection we will develop a sufficient condition for stability of platoon of vehicles.

4.1 Platoon Stability

In this section we will establish the conditions the supervisory and regulation layer controllers have to follow to guarantee the stability of platoon of vehicles. We will use the following definition for platoon stability.

Definition 4.1 *A platoon of vehicles of length n is called stable if* $\|\delta_i(t)\|_\infty \leq \|\delta_{i-1}(t)\|_\infty$ *and* $\|V_{r_i}(t)\|_\infty \leq \|V_{r_{i-1}}(t)\|_\infty$, $i = 2 \ldots n$, *where* δ *is the deviation from the desired spacing and* V_r *is the relative speed between two vehicles.*

Before we analyze the stability of platoon, we will make the following assumption.

Assumption:

A–I Speed fluctuations between any two successive vehicle in the platoon are within the limit Δ_2 defined for the leading vehicle to be a valid target, i.e., $V_{c_i} = V_{i-1}$.

By using Definition **4.1** and assumption **A–I,** the following theorem establishes the conditions for platoon stability.

Theorem 4.2 *Under assumption* **A–I,** *a platoon of vehicles is stable if:*

$$\lambda_0(\max\{1, \hat{b}(k_2 + k_3)\}) \leq \alpha_0.$$

Where λ_0, α_0, $\hat{b}$, k_2 *and* k_3 *are as defined in Theorem 4.1.*

Proof: With supervisory controller in the loop.we have, $\delta_i(s) = G_\delta(s)V_{c_i}$, using assumption **A–I** we have, $\delta_i(s) = G_\delta(s)V_{i-1}$. The transfer function relating δ_i and δ_{i-1} can be found as:

$$\begin{aligned} \frac{\delta_i(s)}{\delta_{i-1}(s)} &= \frac{\delta_i(s)}{V_{i-1}(s)} W_1(s) \frac{V_{i-2}(s)}{\delta_{i-1}(s)}, \\ &= W_1(s), \end{aligned} \tag{53}$$

where $V_i(s) = W_1(s)V_{i-1}(s)$. Similarly, we can show that $\frac{V_{r_i}(s)}{V_{r_{i-1}}(s)} = W_1(s)$. Hence a sufficient condition for platoon stability is that:

$$\|w_1(t)\|_1 \leq 1. \tag{54}$$

From the closed loop system (47) we have:

$$\begin{aligned}\dot{X}_{r_i} &= V_{i-1} - V_i, \\ \ddot{V}_i &= -(\hat{a} + \hat{b}k_1 + \hat{b}k_2\bar{h}_c)\dot{V}_i - (\hat{b}k_2 + \hat{b}k_3 + \hat{b}k_4\bar{h}_c)V_i - (\hat{a} + \hat{b}k_1)\dot{V}_{i-1} \\ &\quad +(\hat{b}k_2 + \hat{b}k_3)V_{i-1} + \hat{b}k_4X_{r_i} - (\hat{b}k_4h_\Delta V_i + \hat{b}k_2\dot{h}_\Delta V_i + \hat{b}k_2h_\Delta\dot{V}_i).\end{aligned} \tag{55}$$

Since $W_1(s)$ is the transfer function between V_i and V_{i-1}, *(55)* can be written **as:**

$$\begin{aligned}\dot{X}_1 &= [A + D_1(t)]X_1 + b_1u_1, \\ y_1 &= c_1X_1,\end{aligned} \tag{56}$$

where $X_1 = [X_{r_i}, V_i, \dot{V}_i]^\mathsf{T}$, $u_1 = V_{i-1}$ and $y_1 = V_i$. The matrices A, $D_1(t)$ are the same **as** defined in (48). The vectors b_1 and c_1 **are:**

$$b_1 = \begin{bmatrix} 1 & 0 & \hat{b}(k_2 + k_3) \end{bmatrix}^\mathsf{T};\ c_1 = \begin{bmatrix} 0 & 1 & 0 \end{bmatrix}.$$

As proved in Theorem **4.1** that $\dot{X}_1 = [A + D_1(t)]X_1$ is u.a.s. and

$$\|y_1\|_\infty \leq \frac{\lambda_0 a_1}{\alpha_0}\|u_1\|_\infty + \epsilon. \tag{57}$$

Since $\|w_1\|_1 = \|T\|_\infty$, where T is the map, $T : u_1 \to Tu_1 = y_1$, we have:

$$\|w_1\|_1 \leq \frac{\lambda_0 a_1}{\alpha_0}. \tag{58}$$

Since $a_1 = \|b_1\|_\infty = \max\{1, \hat{b}(k_2 + k_3)\}$, the sufficient condition for platoon stability is:

$$\lambda_0(\max\{1, \hat{b}(k_2 + k_3)\}) \leq \alpha_0. \tag{59}$$

□

It should be noted that the condition (59) puts a limit on the closed loop poles of PID controller and the choice of filter $C_2(s)$.

5 Simulation and Experimental Results

The automatic vehicle following **(AVF)** controller designed in section three is simulated using the PID throttle/brake controller designed in [10] and a nonlinear longitudinal vehicle model [10]. The values chosen for different design constants in the supervisory controller are given below:

$h_t = 2$ sec, $\Delta_1 = 2.5$ mph, $\Delta_2 = 5$ mph. (see (3)),

$h_m = 1.2$ sec, $h_{min} = 0.25$ sec, $h^d_{max} = 1.5$ sec, $V_{max} = 65$ mph. (see (9), (10)),

$k_p = 0.1$, $\Delta h = 0.02$, $k_i = 10$. (see (12), (6) and (16)),

$A_{max} = 0.7$, $A_{min} = -0.4$, $A'_{max} = 0.7$, $A'_{min} = -2$. (see (20) and (21)),

$V_s = 55$ mph. (see (17)).

The design constants for the throttle/brake controller [10] and the constraints for maximum acceleration, deceleration and jerk are chosen as:

$\omega_n = 0.1$, $\zeta = 1$, $\lambda_0 = 1.2$,

$k_5 = 1$, $k_6 = 0.25$,

$a_{max} = 0.2$g, $a_{min} = -0.2$g, $j_{max} = 10\ m/sec^3$.

The logic switch designed for throttle and brake controller [10] requires three parameters, X_{min}, X_{max} and V_1. The values chosen for these parameters are:

$X_{min} = 6$ m, $X_{max} = 40$ m, $V_1 = 13.4$ m/sec.

Three different tests are simulated to investigate the performance of the designed controller under different operating conditions, these are given in the subsections below. Finally, the test results of automatic vehicle following demonstrated in an actual highway environment are briefly discussed in subsection **5.4.**

5.1 Test 1: Leader-Follower Scenario

In this test the cooperative driving mode is simulated, only two vehicles are used and are designated as the leader and follower. The effect of different initial conditions while switching on the AVF is studied. In this scenario the leader is assumed to be in the AVF mode at $t = 0$ sec, and is traveling at a speed of 55 mph, which is the roadway commanded speed, i.e., $V_l = V_R = 55$ mph. The follower, however, switches on the **AVF** with different initial conditions. The cases used for simulation are:

T1–I $V_f = 45$ mph $< V_l$, $h_f = h_R = 0.8$ sec.

T1–II $V_f = V_R$, $h_f = 0.6$ sec. $< h_R$.

The simulation results for these cases are shown in Figures **15-16.** It can be seen that the following vehicle manages to operate in the automatic following mode even though starting from significantly different initial conditions. The magnitude of the transients are quite small, maximum acceleration and deceleration are limited to **0.16g** and -0.15g respectively. The maximum jerk is observed in Figure 16, where the following vehicle executes a slowing down maneuver to increase the headway, the value of maximum jerk is **3.6** m/sec^3.

5.2 Test 2: Leader-Follower Scenario: Effect of Roadway Commands

In this test the same leader-follower scenario of Test 1 is assumed, i.e., the leader and follower are traveling at roadway commanded speed, $V_l = V_f = V_R = 55$ mph, and $h_f = h_R = 0.8$ sec. In the following cases it is assumed that at $t = 60$ sec, the roadway changes speed and/or headway commands. The cases are:

T2–I $V_R(k_0) = 65$ mph $> V_R(k_0 - 1)$, where $k_0 T = 60$ sec.

T2–II $h_R(k_0) = 1.0$ sec $> h_R(k_0 - 1)$

The simulation results for these cases are shown in Figures 17-18. In Figure 17, both vehicles accelerate from a steady speed of 55 mph to **65** mph, following the roadway command issued at $t = 60$ sec. The maximum acceleration for both vehicles is limited to about 0.05g. In Figure **18,** the following vehicle decreases its speed momentarily to increase the headway from 0.8 sec to 1.0 sec. It should be noted that a change in the desired headway at $t = 60$ sec, creates a negative position error, the throttle/brake controller uses this new headway command to decrease the position error.

5.3 Test 3: Platoon Maneuvers

In the third set of simulations, a platoon of six vehicles is used to demonstrate the process of platoon formation and deformation. Furthermore, the effects of acceleration and deceleration on the platoon stability is also analyzed. The cases used for simulations are:

T3–I Platoon formation: Five vehicles join the leader at a consecutive interval of 5 sec.

T3–II Platoon deformation: Vehicles exit from the end of the platoon at a consecutive interval of **5** sec.

T3–III Platoon acceleration/deceleration: In steady state at **55** mph, platoon accelerates/decelerates to **65/45** mph.

The results of these simulations are shown in Figure 19-22. In the platoon formation maneuver, Figure 19, the incoming vehicles were made to join the platoon with monotonically increasing negative position error. The magnitude of speed overshoot is reasonably small even with large negative position error. In the case of platoon deformation, Figure 20, at the time the AVF is switched off, the headway is gradually increased from $h_R = 0.8$ sec to $h_{max} = 1.2$ sec at a rate of **0.02** sec **for** each sampling interval. Hence at a speed of 55 mph it creates a position error of about **-1.2** m during this period of time. The position error goes to zero **as** the **AVF** is switched off.

When the platoon executes an acceleration maneuver, Figure 21, the speed increases from 55 mph to **65** mph, with no slinky type effect. For the deceleration maneuver, as pointed out earlier, the condition for following target given in **(3)** and switching the desired speed from the leader speed V_l to the roadway speed V_R in (20), if the former is significantly different than the later, helps in uniform deceleration of platoon. Hence all of the vehicles uniformly decelerate till the speed of the leading vehicles is within $\Delta_1 = 2.5$ mph of V_R, at which point the leading vehicles are treated **as** valid targets.

5.4 Experiments on 1-15

In this experiment, two vehicles were used. Each of the two vehicles were equipped with ranging sensors, which can measure relative distance up to about 20 meters, and v-v communication devices. Through the communication, the leading vehicle passes its speed, acceleration, and other information to the following vehicle. The vehicles were equipped with the throttle actuators only, hence the desired speed profiles were chosen so that the required deceleration can be achieved without using brakes (by using engine torque only).

For each controller designed in [10], tests were conducted with two kind of time headway, 0.25 seconds and 0.4 seconds. There were **3** speed profiles for the Ieading vehicle. The first speed profile was starting at **30** mph, going to 60 mph with small acceleration, staying at 60 mph for a while, decreasing to **40** mph slowly, going **back** to 60 mph slowly, and then staying at 60. For simplicity, we use 30-60-40-60 to indicate this speed profile. The second speed profile is 40-50-40-50 or 40-50 with large acceleration. The third speed profile is that the leading vehicle **was** driven manually following some sinusoidal speed curve. The experimental results of some of the tested controllers are included here, for a detailed description of this test conducted on 1-15 the reader is referred to [17].

The test results of nonlinear PID throttle controller and no v-v communication are shown in Figures **23-24.** It can be seen from Figure 24 that the negative position error is within 1 m, which allows the following vehicle to travel close to the leading vehicle without any collision. The speed.profiles in Figure **23** show that the following vehicle tracks the speed profile of the leading vehicle closely except near transitions, where a sudden change in speed of the leading vehicle creates a large position error which is reduced by making the speed of the following vehicle greater than that of the leading vehicle during that interval. In this test the headway is set to be 0.25 seconds, hence as shown in Figure 24 the actual headway is smoothly reduced from an initial value of 0.265 seconds to the desired value of 0.25 seconds. **As** pointed out earlier that the controller design ensures that the acceleration of the vehicle is within the specified bounds. The claim is obvious from the acceleration profiles shown in Figure **23,** where the acceleration of the following vehicle is less than the set limit of $1 m/sec^2$, even though the leading vehicle accelerates beyond the set limit.

The test results of PID controller with communication for a speed profile of 40-55-40-55 are shown in Figures 25-26. By comparing Figure 25 with Figure **23** it is obvious that the addition of v-v communication has helped the following vehicle to closely track the speed profile of the leading vehicle. Hence transmission of the acceleration of leading vehicle reduces the time delay incurred by assessing the same information through the sensor measurements. Similarly Figure 26 shows that the maximum negative position error is close to 1 m, which is satisfactory considering the fact that no brake actuator was used in the experiment and the required deceleration was obtained by the engine torque only.

Figures 27-28 and **29-30** show the experimental results for adaptive controller without and with v-v communication respectively. In both cases sinusoidal speed profile, which represents typical manual driving, was chosen. The time headway in both cases was selected to be 0.25 seconds. Again by comparison of Figures 27 and 29 it is obvious that addition of v-v communication improves the performance of the vehicle following controller.

6 Conclusion

In this paper we have designed and tested a vehicle control system for achieving full vehicle automation in the longitudinal direction. The vehicle control system is an interconnection of a supervisory controller and a throttle/brake controller. The supervisory controller is designed so that it can operate in different configurations of AHS, allowing the vehicle to operate with varying distribution of authority between the driver and external agents. The supervisory controller helps the driver during transitions and generates the desired trajectory of the vehicle based on available inputs. Overall system safety is improved by inclusion of emergency situation handling algorithm **as** a part of supervisory controller. The simulation results of some of the basic vehicle following maneuvers are used to test the performance of the designed controllers. Finally, the experimental results of a vehicle following test conducted on 1-15 verifies the system performance in an .actual highway environment.

Acknowledgment:

We thank Dr. Z. Xu for his useful comments and help for this study.

Re'ferences

[1] *Y*. Sun, P. Ioannou, **"A** Handbook for Inter-Vehicle Spacing in Vehicle Following," California PATH Research Report, UCB-ITS-PRR-95-1

[2] D. B. Maciuca, **J.** K. Hedrick, "Brake Dynamics Effect on AHS Lane Capacity," Systems and Issues in ITS, **SAE,** Warrandale, **PA,** pp. 81-86, 1995.

[3] V. Sarakki, J. Kerr, "Effectiveness of IVHS Elements on Freeway/Arterial Capacity: Concepts and Case Studies," 64th Meeting of Institute of Transportation Engineers, Dallas, Compendium of Technical Papers, Institute of Transportation Engineers, Washington D.C., pp. **303-307,** 1994.

[4] M. Shannon, et al., "Precursor Systems Analyses of Automated Highway Systems: AHS Safety Issues," vol. 9, Federal Highway Administration, Washington D.C., Report no. FHWA-RD-95-105, 1995.

[5] A. Hitchcock, "Configuration and Maneuvers in Safety-Consciously Designed AHS Configuration," California PATH Program, University of California at Berkeley, UCB-ITS-PWP-95-2, 1995.

[6] K. S. Chang, J. K. Hedrick, W. B. Zhang, P. Varaiya, M. Tomizuka, S. E. Shladover, "Automated Highway System Experiments in the PATH Program", *IVHS Journal*, vol 1, no. 1, pp. 63-87, Apr. 1993.

[7] C. C. Chien, P. Ioannou, "Automatic Vehicle Following", *Proc. of 1992 American Control Conference,* Chicago, IL, pp. 1748-1752. June 1992.

[8] J. K. Hedrick, et. al, "Control Issues in Automated Highway Systems", *IEEE Control Systems,* vol. 14, no. 6, pp. 21-32, Dec. 1994.

[9] P. Ioannou, C. C. Chien, "Intelligent Cruise Control", *IEEE Transactions on Vehicular Technology,* vol. 42, no. 4, pp. 657-672, Nov. 1993.

[10] P. Ioannou, Z. Xu, "Throttle and Brake Control System for Automatic Vehicle Following", *IVHS Journal*, vol. 1(4), pp. 345-377, 1994.

[11] S. E. Shladover, et. al, "Automatic Vehicle Control Developments in the PATH Program", *IEEE Transactions on Vehicular Technology,* vol. 40, no. 1, pp. 114-130, Feb. 1993.

[12] C. C. Chien, Y. Zhang, A. Stotsky, S. R. Dharmasena, P. Ioannou, "Macroscopic Roadway Traffic Controller Design", California PATH Research Report, UCB-ITS-PRR-95-28.

[13] P. Varaiya, "Smart Cars on Smart Roads: Problems of Control", *IEEE Transactions on Automatic Control,* vol. 38, no. 2, pp. 195-207, Feb. 1993.

[14] J. K. Hedrick, D. McMahon, V. Narendran, D. Swaroop, "Longitudinal Vehicle Controller Design for IVHS System," *Proc. of ACC,* vol. 3, pp. 3107-3112, June 1991.

[15] A. S. Hauksdottir, R. E. Fenton, "On the Design of a Vehicle Longitudinal Controller," *IEEE Trans. on Vehicular Technology,* vol. VT-34, no. 4, pp. 182-187, Nov. 1985.

[16] W. A. Coppel, "Stability and Asymptotic Behavior of Differential Equations", D. C. Heath and Company, Boston, pp. 64-70, 1965.

[17] P. Ioannou, Z. Xu, H. Raza, "Report on 1-15 Vehicle Following Test", USC-CATT Report #96-3-01.

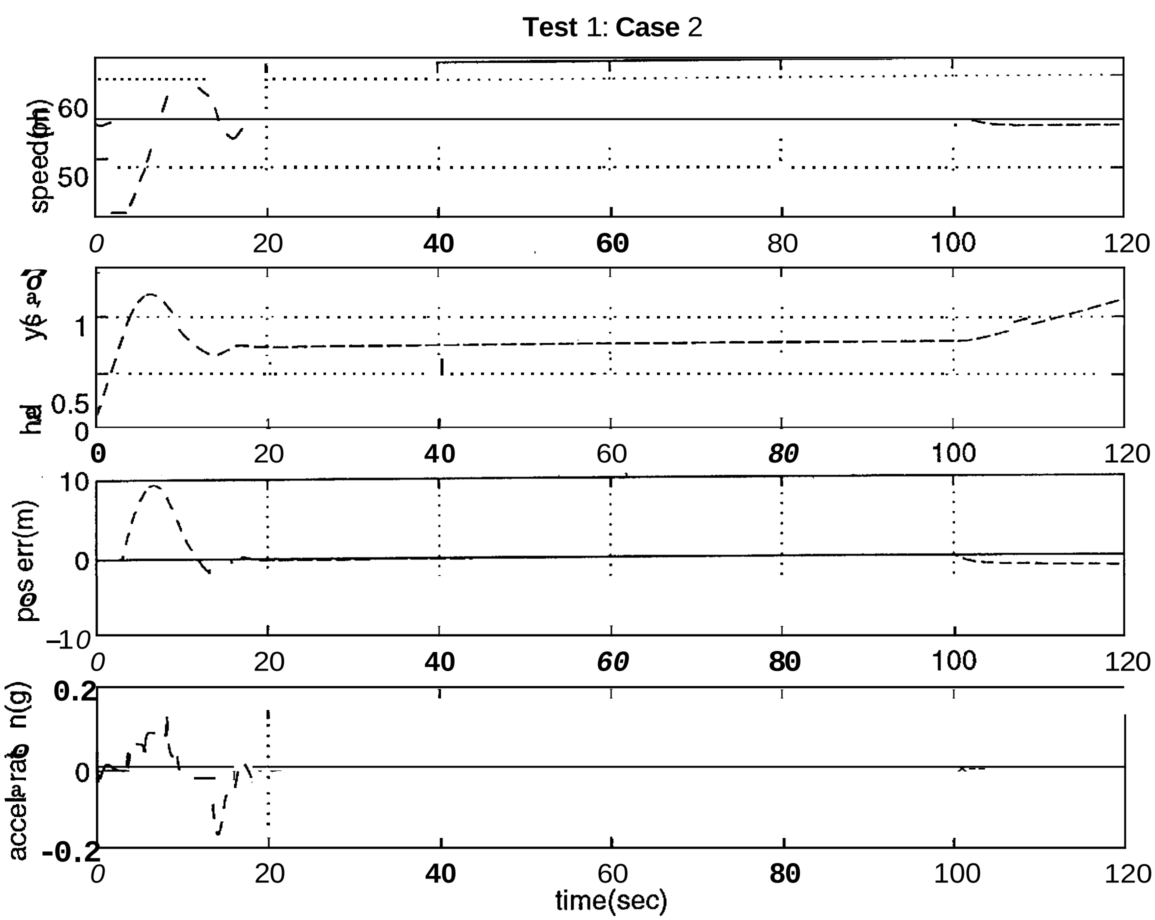

Figure 15: Follower switches on AVF at $t = 3$ sec with $V_f = 45$ mph and $h_f = h_R = 0.8$ sec. AVF is switched off at $t = 100$ sec.

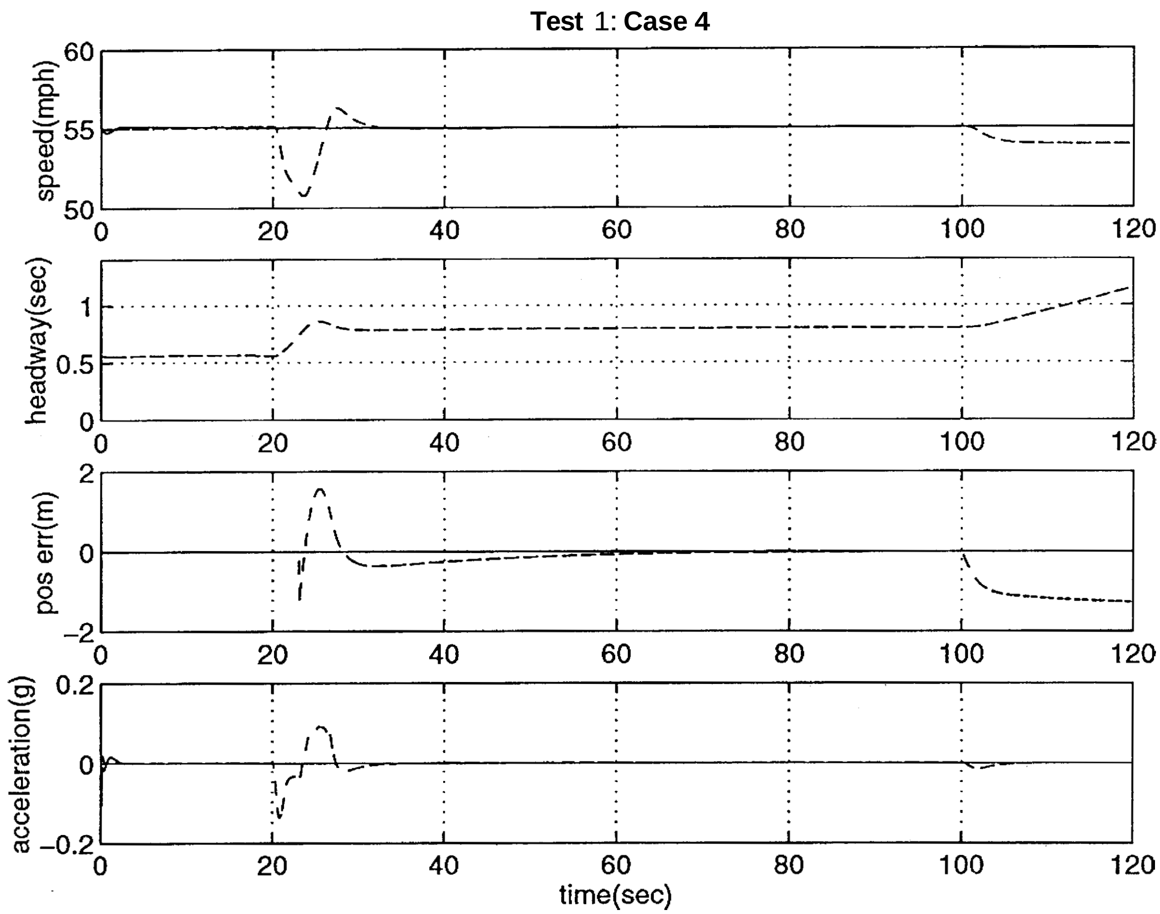

Figure 16: Follower switches on AVF at $t = 20$ sec with $V_f = 55$ mph and $h_f = 0.6$ sec. AVF is switched off at $t = 100$ sec.

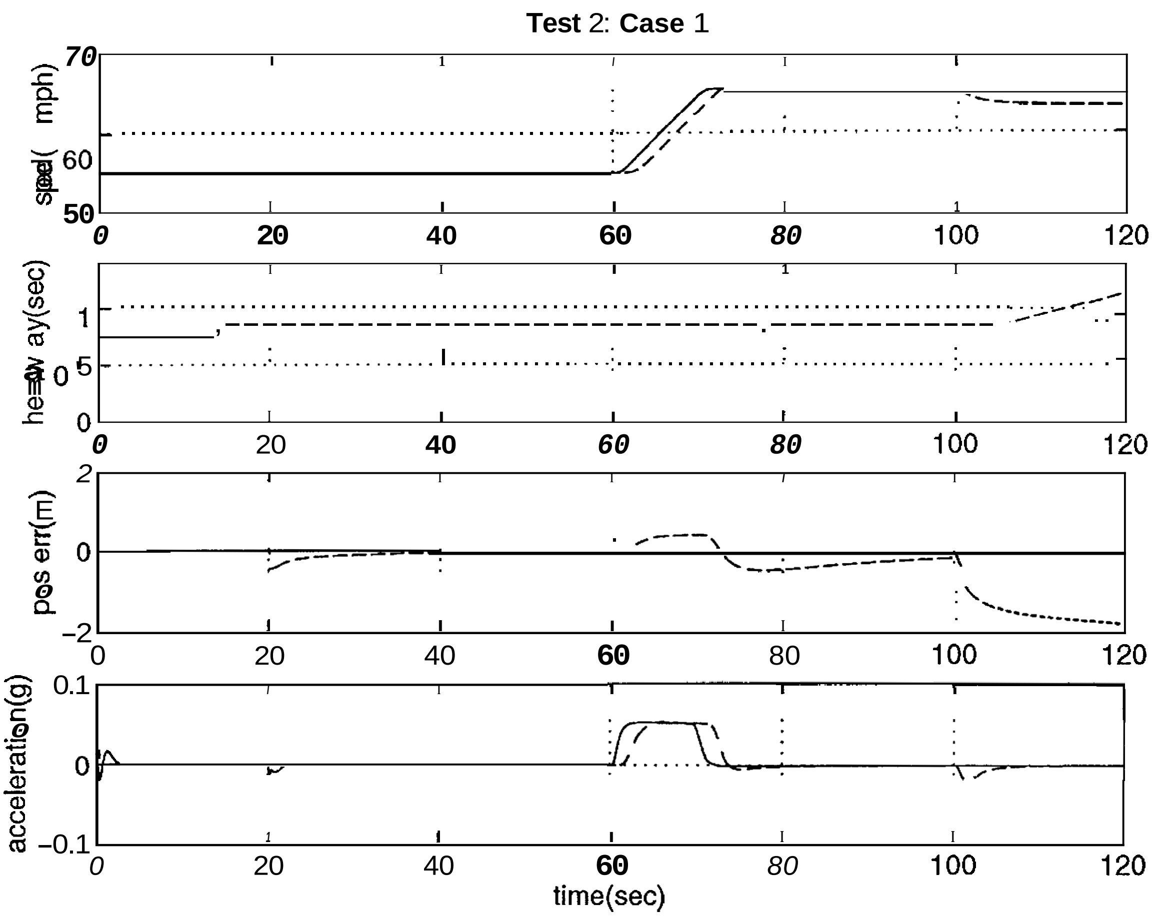

Figure 17: **At** $t = 60$ sec V_R changes from **55** to 65 mph.

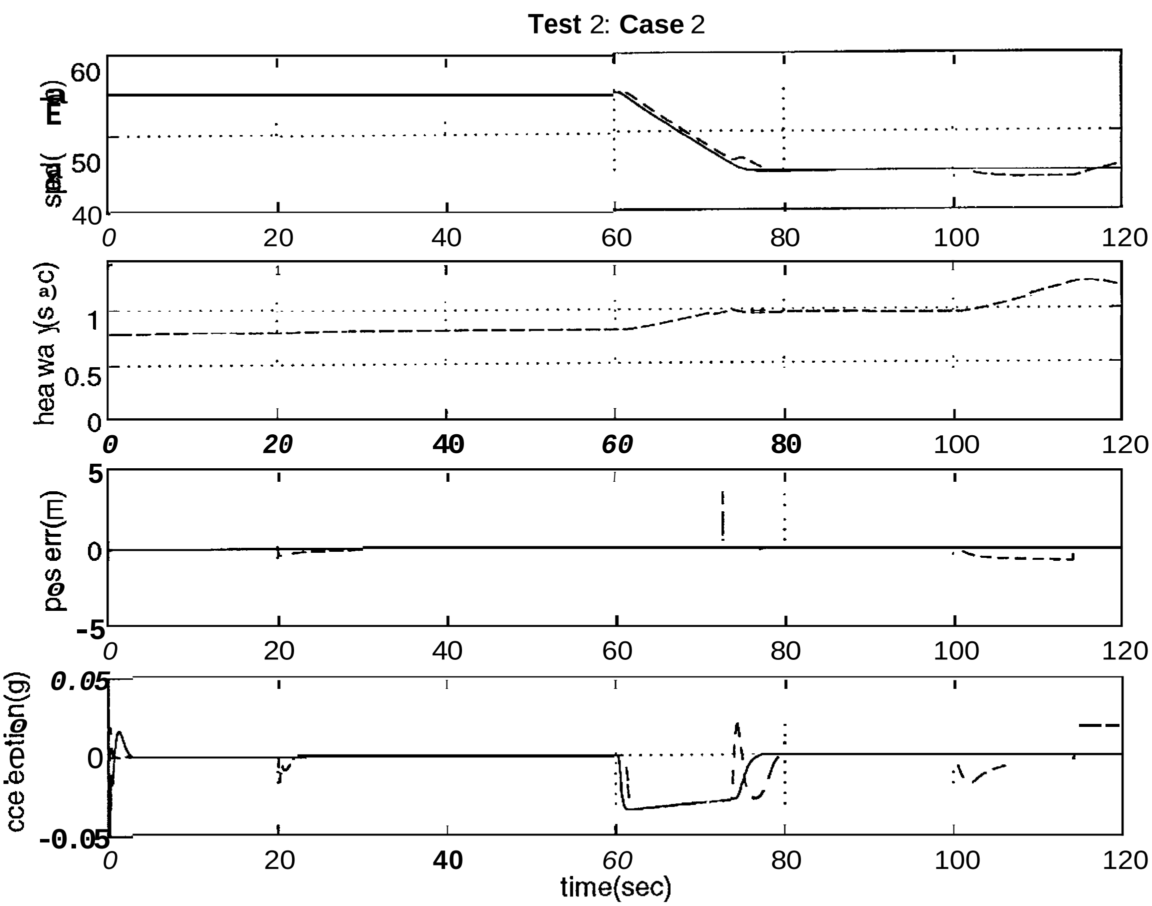

Figure 18: At $t = 60$ sec, h_R changes from 0.8 to 1.0 sec.

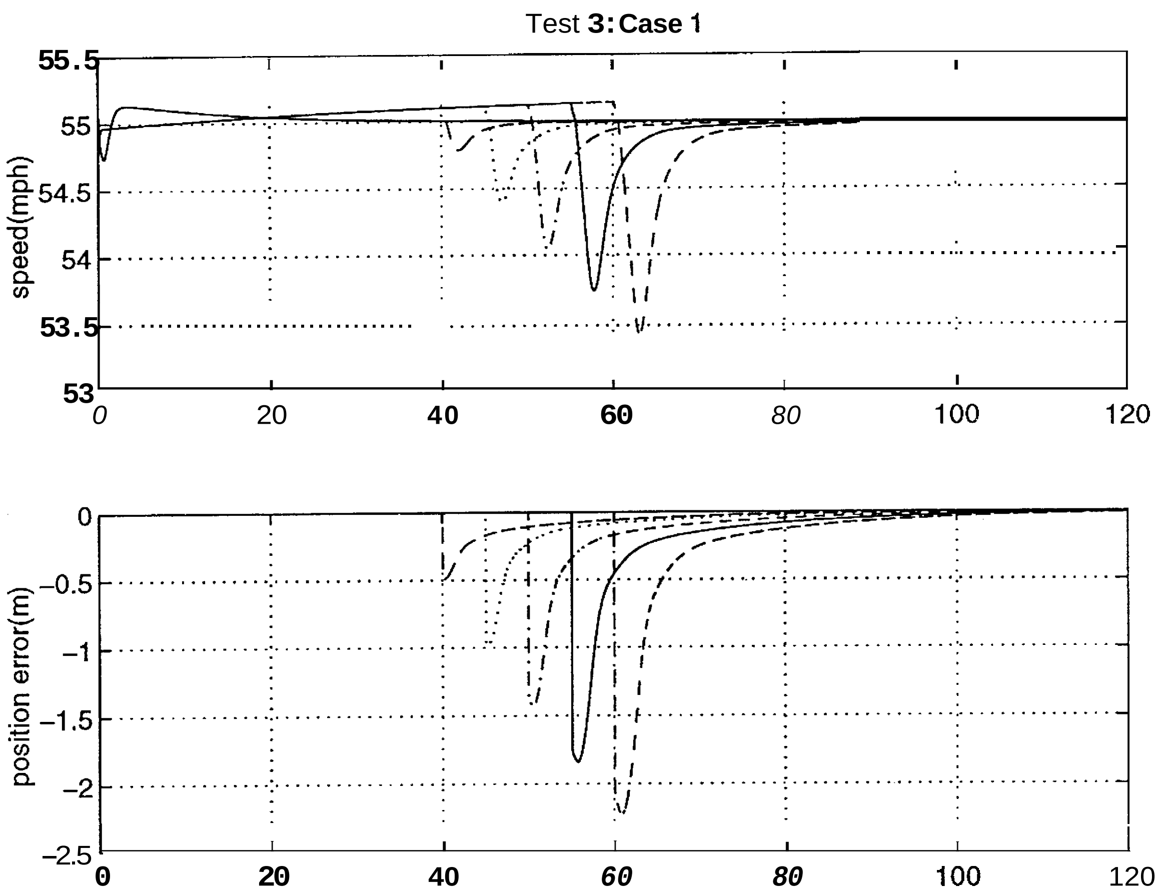

Figure 19: Platoon formation: At $t = 40$ sec, first vehicle joins the leader of the platoon. Four more vehicles join the platoon at a consecutive interval of 5 sec. Platoon formation was stable even though the starting position error was quite large.

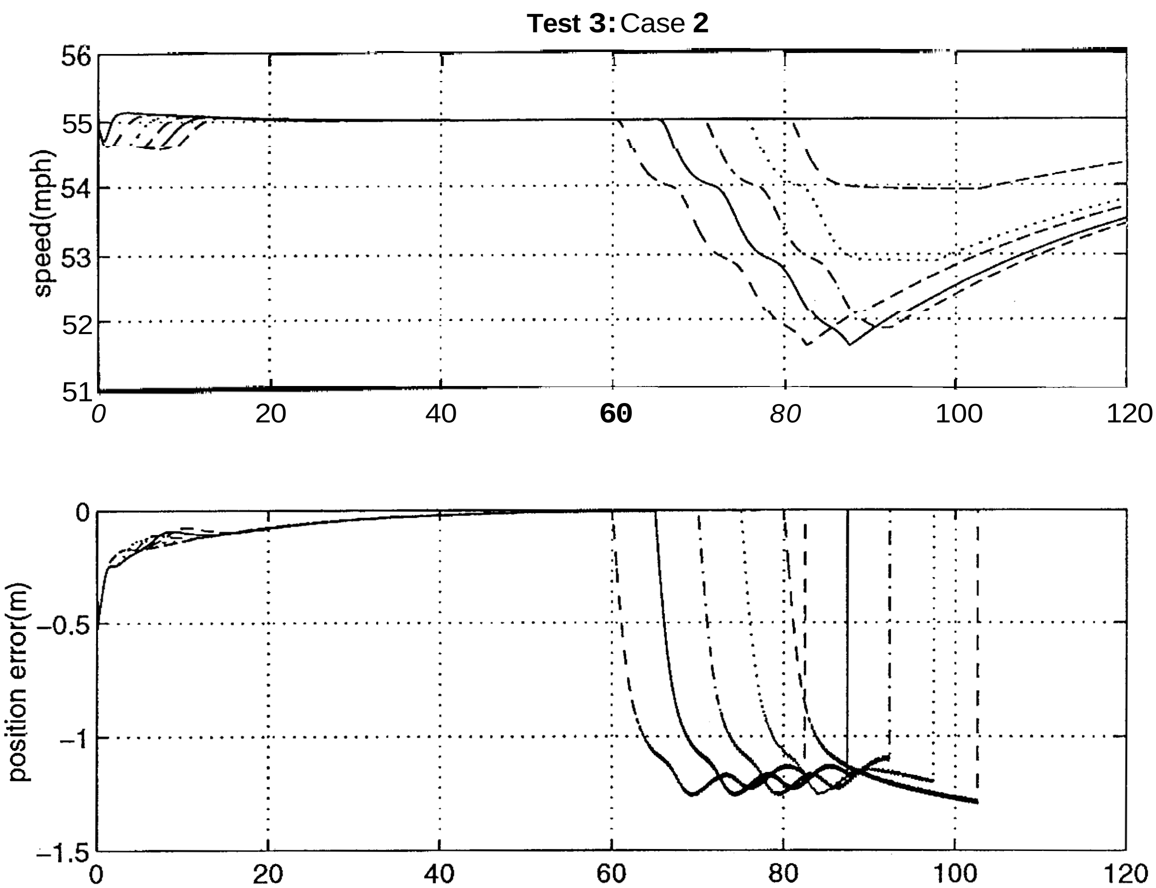

Figure 20: Platoon deformation: At $t = 60$ sec, vehicles start exiting at a consecutive interval of 5 sec. **A** negative position error is due to transition to manual operation, where the headway is increased till it reaches the specified value.

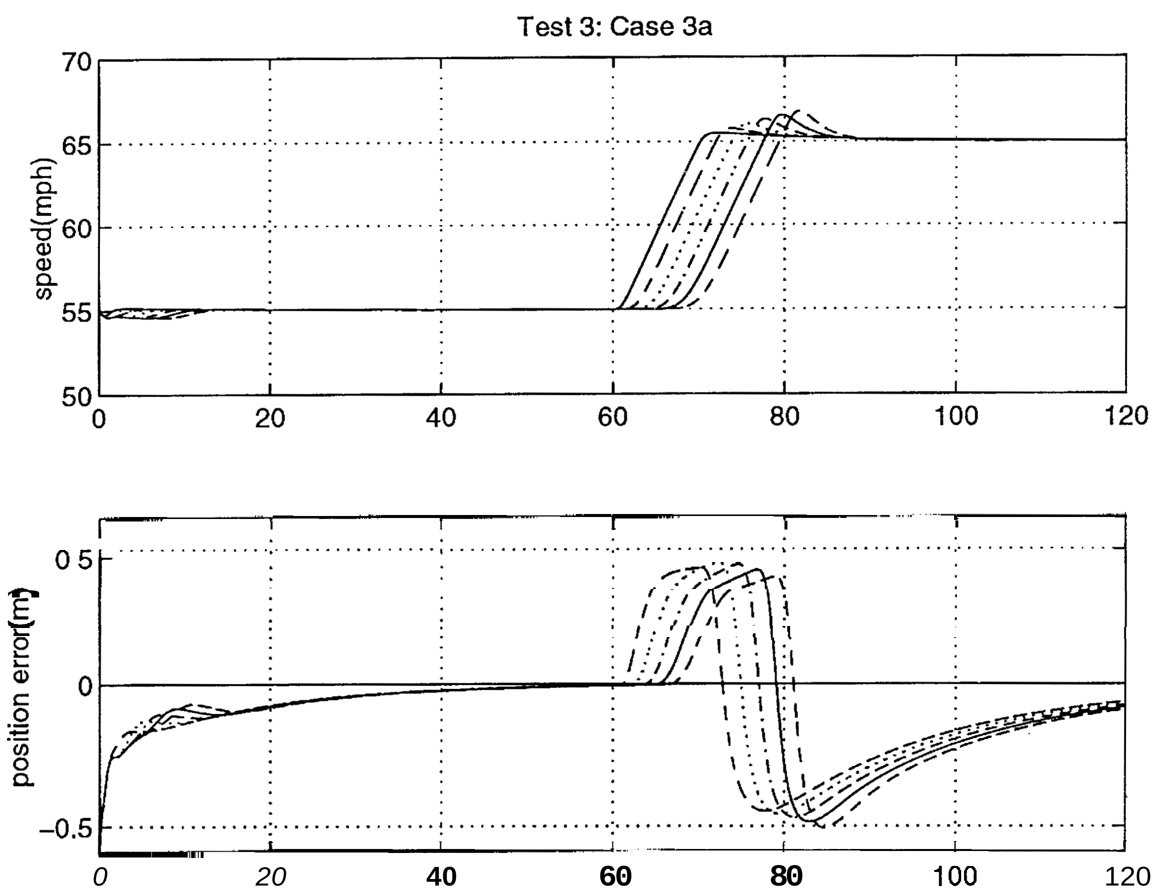

Figure 21: At $t = 60$ sec, platoon accelerates to 65 mph.

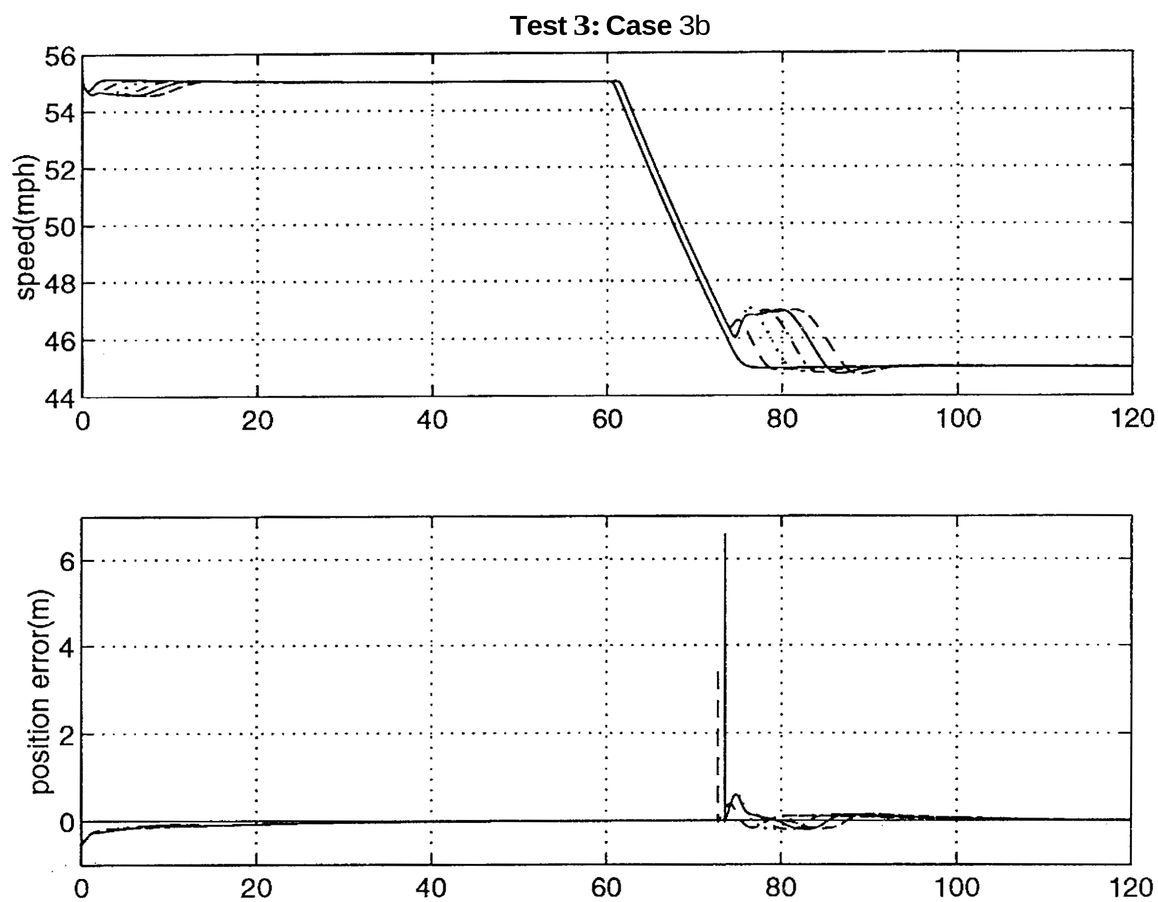

Figure 22: **At** $t = 60$ sec, platoon decelerates to **45** mph.

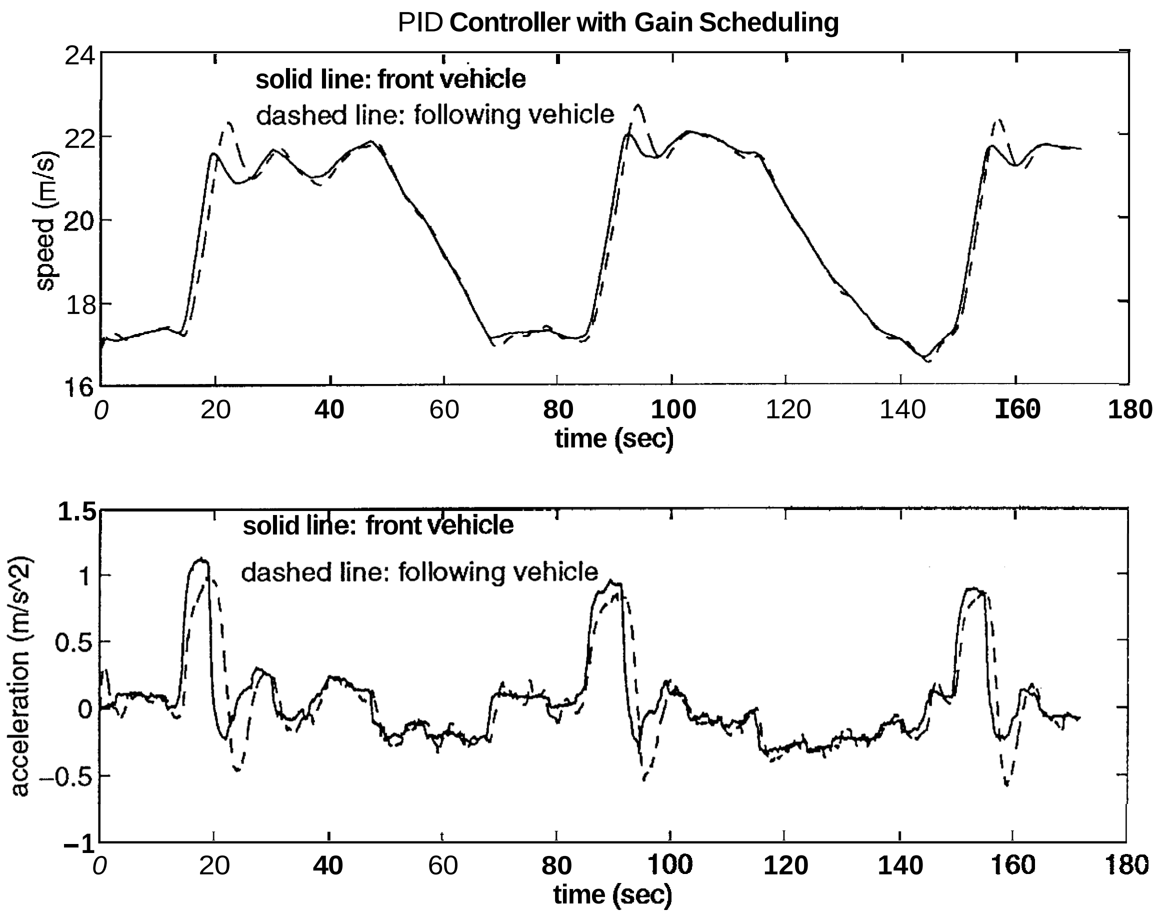

Figure **23:** The speed and acceleration profiles for nonlinear PID controller with no v-v communication. The desired speed profile is **40-50-40-50** with large acceleration.

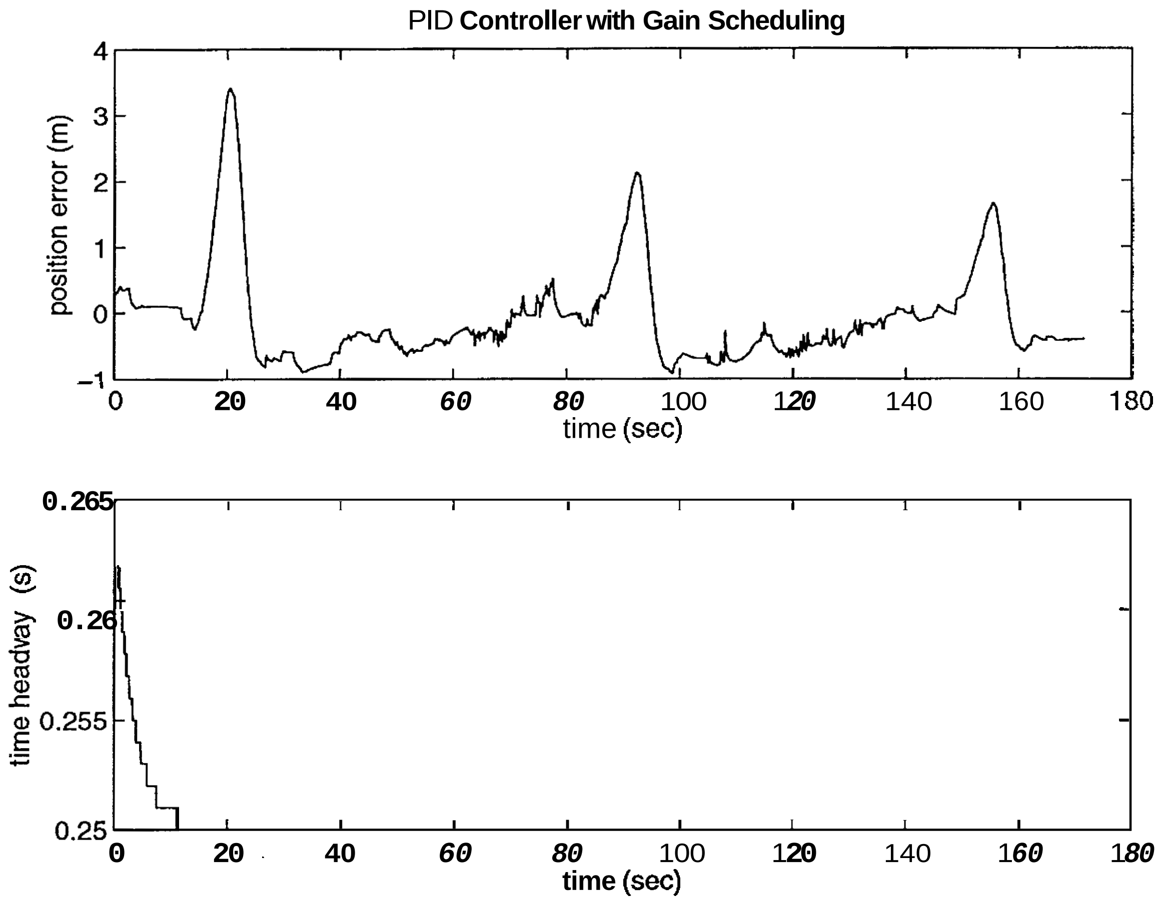

Figure 24: The position error and time headway for nonlinear PID controller with no v-v communication.

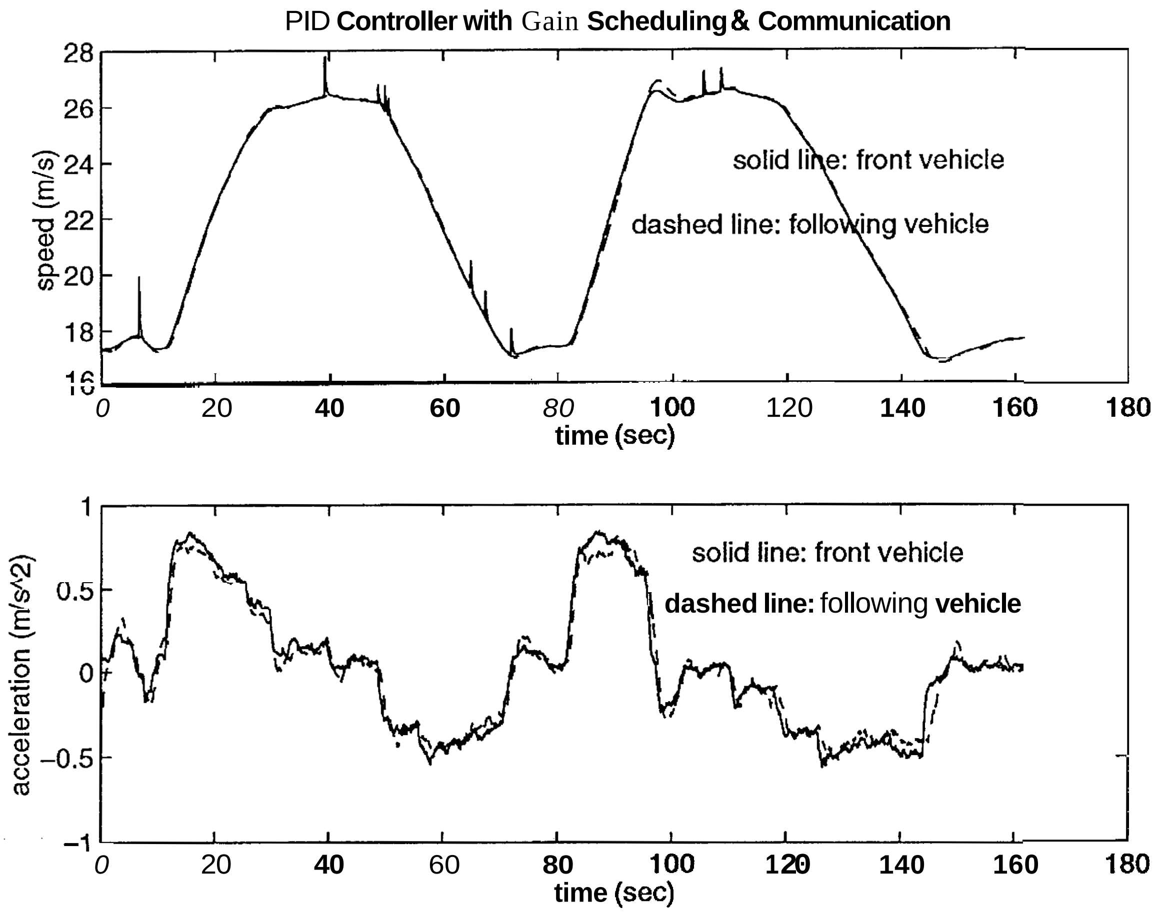

Figure 25: The speed and acceleration profiles for nonlinear PID controller with v-v communication. The desired speed profile is 40-55-40-55 with large acceleration.

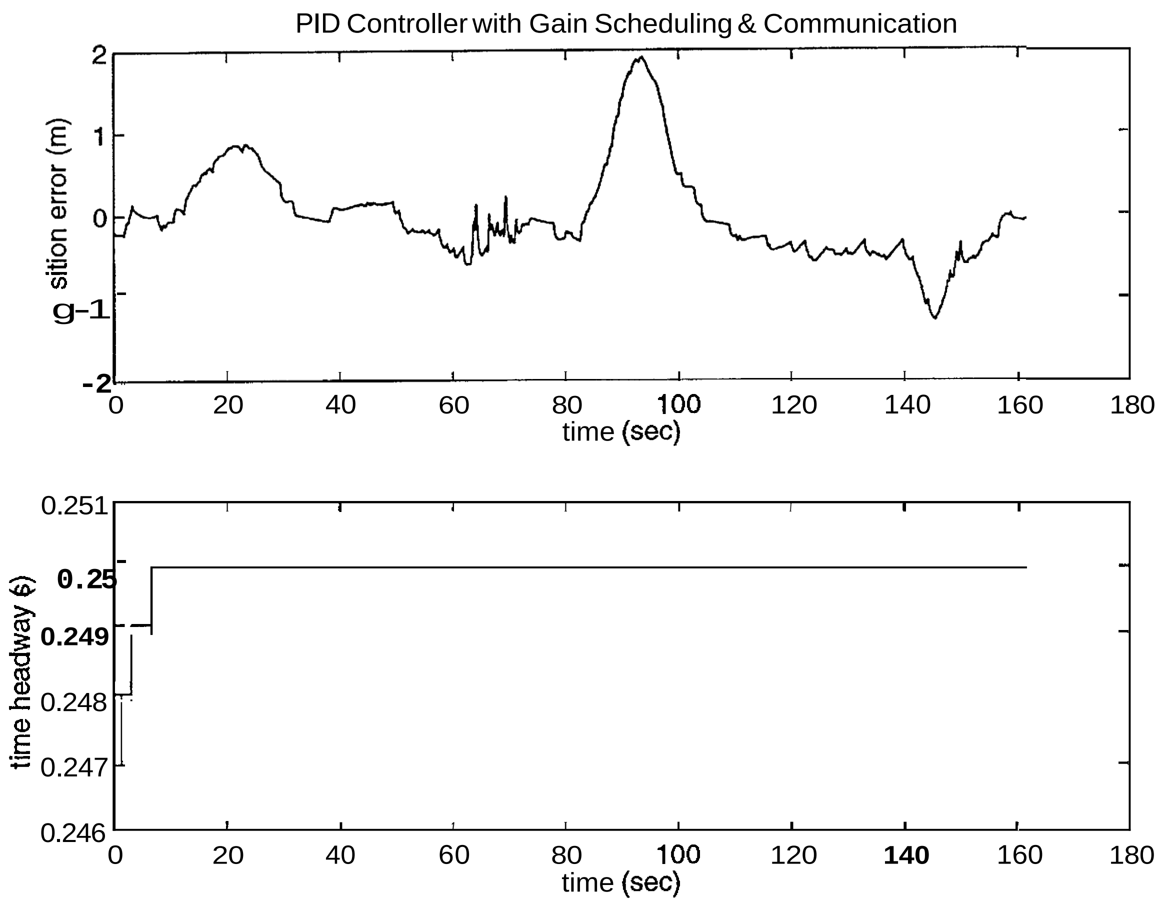

Figure 26: The position error and time headway for nonlinear PID controller with v-v communication.

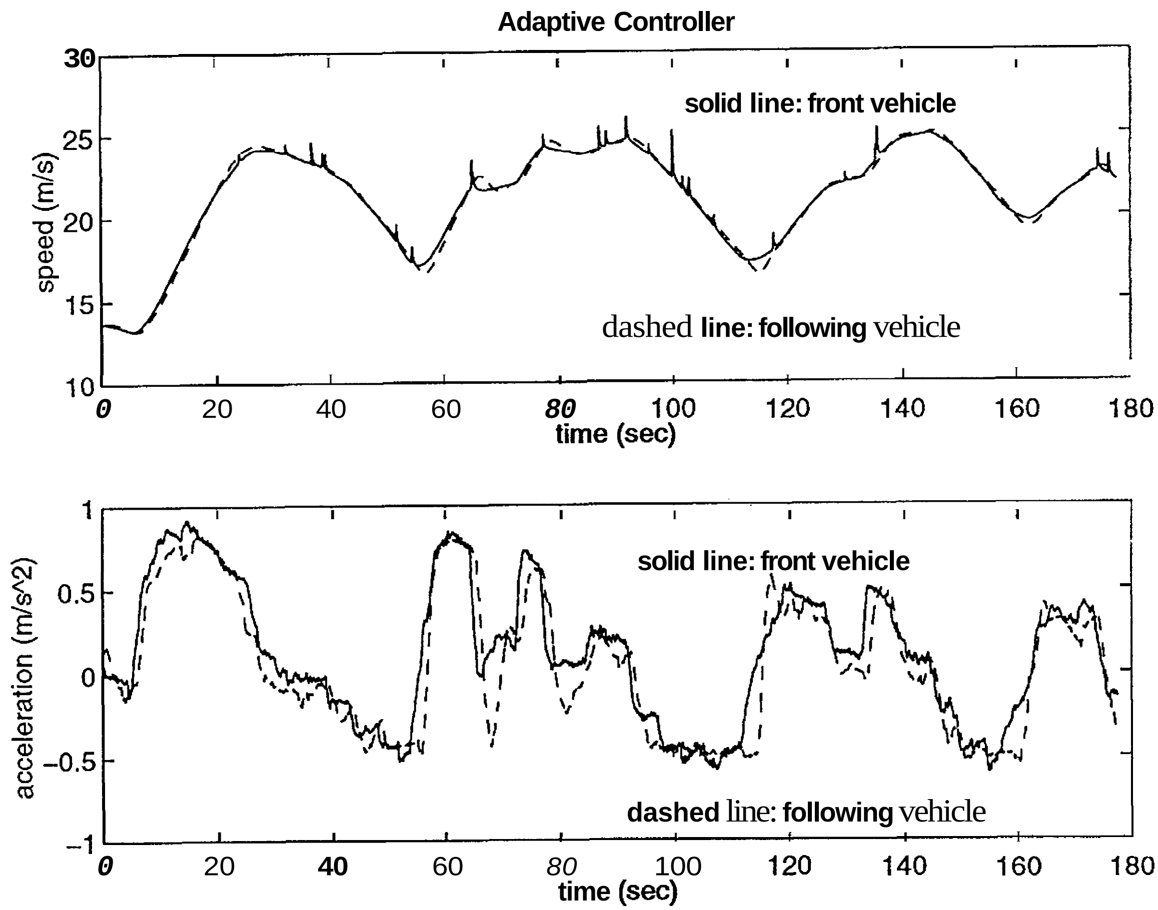

Figure 27: The speed and acceleration profiles for adaptive controller without v-v communication. The sharp spikes in leading vehicle speed **are** due to sensor noise.

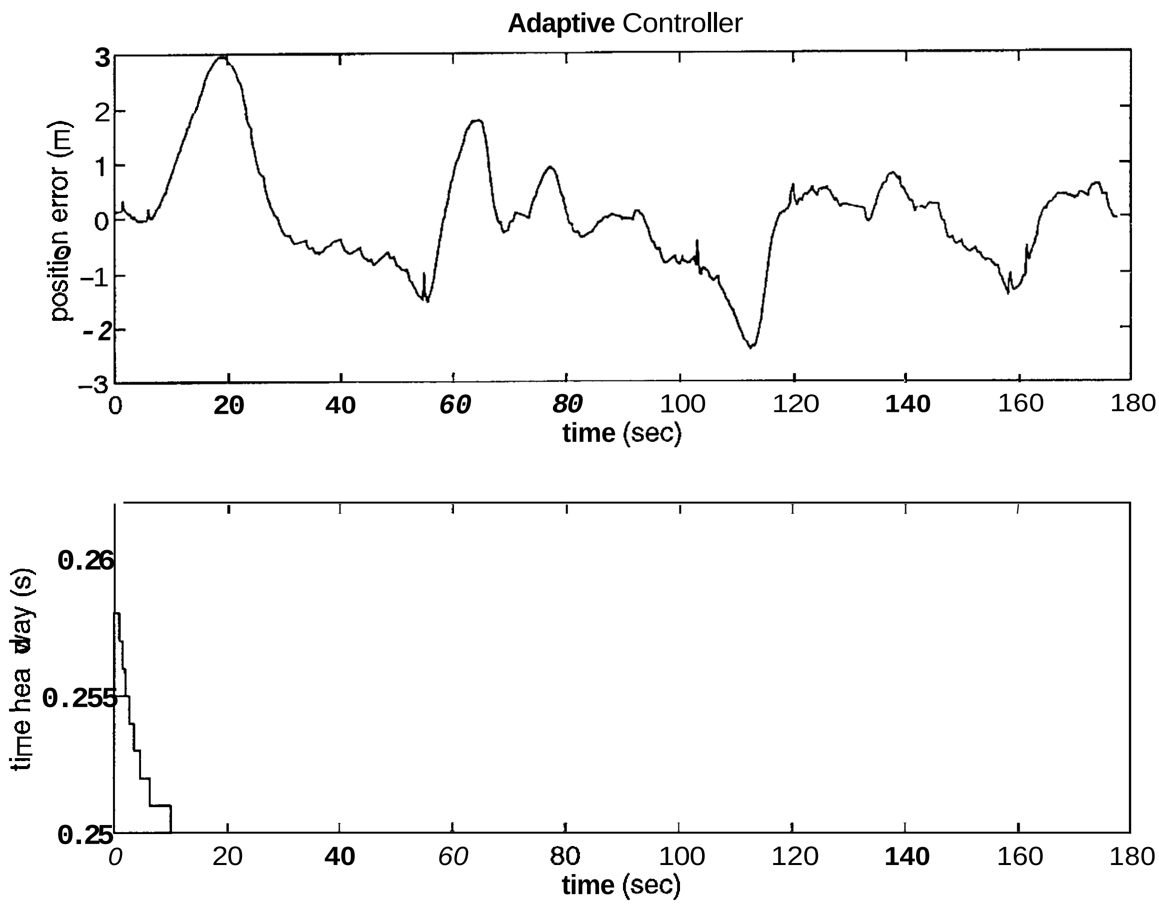

Figure 28: The position error and time headway for adaptive controller without v-v communication.

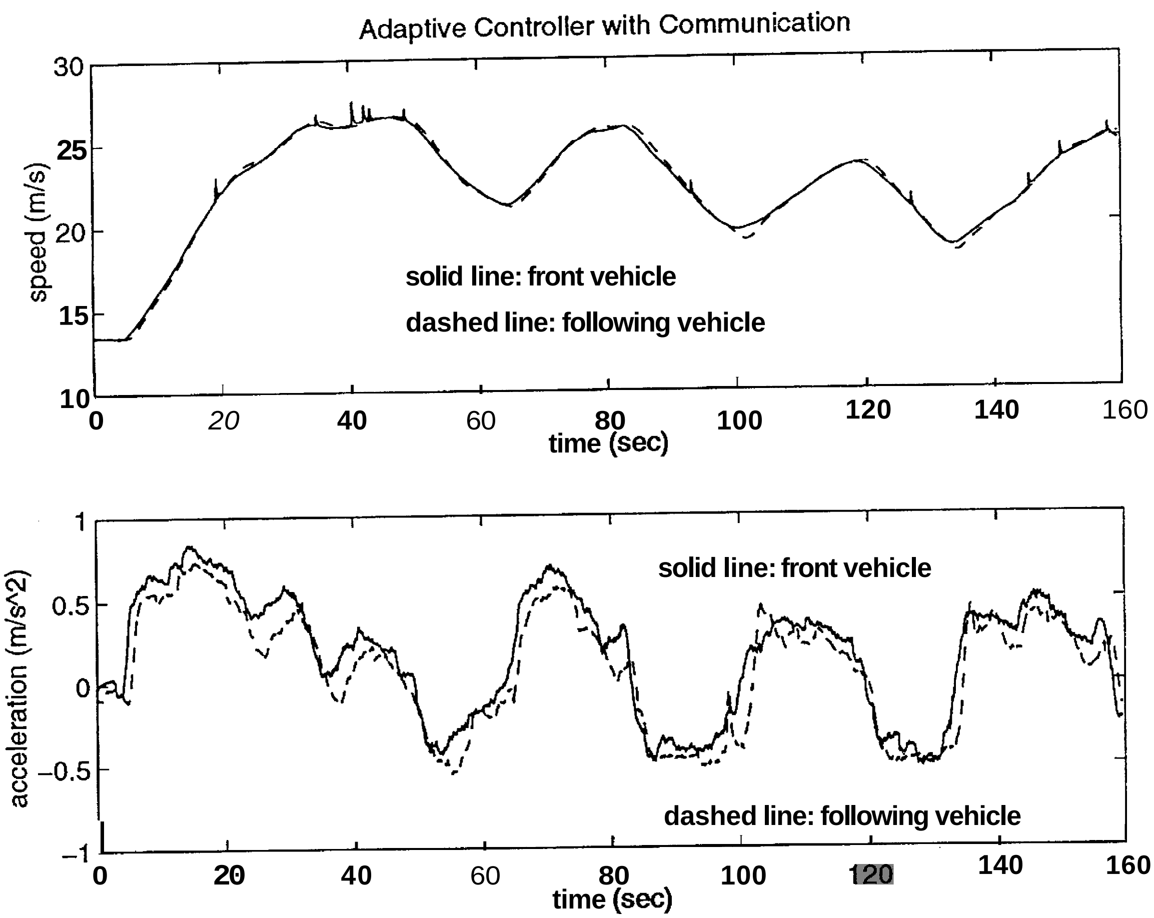

Figure 29: The speed and acceleration profiles for adaptive controller with v-v communication. The sharp spikes in leading vehicle speed are due to sensor noise.

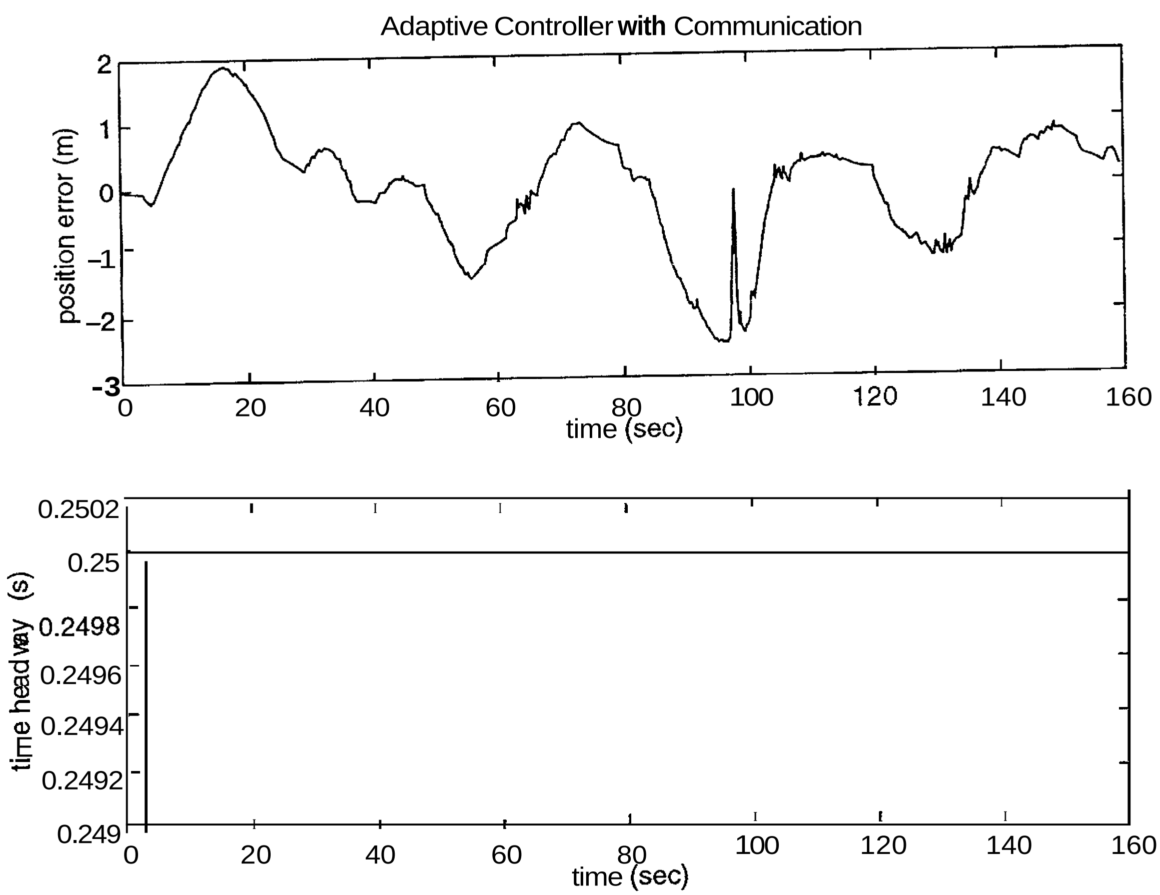

Figure 30: The position error and time headway for adaptive controller with v-v communication.